In silico identification of metabolic enzyme drug targets in *Burkholderia pseudomallei*

Jean F. Challacombe
Bioscience Division, Los Alamos National Laboratory, Los Alamos, NM, 87545

Correspondence: jchalla@lanl.gov

Abstract
The intracellular pathogen *Burkholderia pseudomallei,* which is endemic to parts of southeast Asia and northern Australia, causes the disease melioidosis. Although acute infections can be treated with antibiotics, melioidosis is difficult to cure, and some patients develop chronic infections or a recrudescence of the disease months or years after treatment of the initial infection. *B. pseudomallei* strains have a high level of natural resistance to a variety of antibiotics, and with limited options for new antibiotics on the horizon, alternatives are needed.

The aim of the present study was to characterize the metabolic capabilities of *B. pseudomallei*, identify metabolites and aspects of the metabolic network crucial for pathogen survival, understand the metabolic interactions that occur between pathogen and host cells, and determine if any of the metabolic enzymes produced by the pathogen might be potential antibacterial targets.

This aim was accomplished through genome scale metabolic modeling of *B. pseudomallei* under different external conditions, including all nutrients that could be consumed by the model and only the nutrients available in culture media. Using this approach, candidate chokepoints were identified, then knocked out *in silico* under the different nutrient conditions. The effect of each knockout on the metabolic network was examined. When four of the candidate chokepoints were knocked out *in silico*, the flux through the *B. pseudomallei* network was decreased, depending on the nutrient conditions. These results demonstrate the utility of genome-scale metabolic modeling methods for *in silico* studies of pathogen metabolism and for drug target identification in *B. pseudomallei*.

Introduction

The intracellular pathogen *Burkholderia pseudomallei,* which causes the disease melioidosis, is acquired from the environment in parts of southeast Asia and northern Australia (1, 2). Although acute infections can be treated with antibiotics, melioidosis is difficult to cure, requiring lengthy treatment in two phases for a duration of ~20 weeks (3, 4). Despite antibiotic therapy, some patients have persistent cases that develop into chronic infections, and others experience a recrudescence of the disease months or years after treatment of the initial infection with antibiotics (5). *B. pseudomallei* strains have a high level of natural resistance to a variety of antibiotics (6-8), and with limited options for new antibiotics on the horizon, alternatives are desperately needed.

The availability of many *B. pseudomallei* genomes and advances in computational analysis methods make possible the rapid identification of novel antibacterial targets by selecting the best targets from complete sets of protein coding genes. Previous studies comparing the genomes of bacterial pathogens have demonstrated that essential genes present in pathogen genomes, but not in the host, make the best therapeutic targets (9). Many known antibacterial compounds are enzyme inhibitors (10, 11), so metabolic enzymes specific to bacteria represent promising drug targets (9).

Enzyme targets present in key metabolic pathways have been identified in *B. pseudomallei* and other bacterial pathogens; these pathways include fatty acid biosynthesis (12-14), the glyoxalate shunt (15, 16), the chorismate pathway for biosynthesis of aromatic amino acids (17), purine, histidine, 4-aminobenzoate, and lipoate biosynthesis (18, 19), leucine, threonine, p-aminobenzoic acid, aromatic compound biosynthesis (20), branched chain amino acid biosynthesis (21), purine metabolism (22). Other enzyme targets have been identified that are not in pathways - alanine racemase (interconverts L- and D-alanine) (23), superoxide dismutase (24) and cyclic di-GMP phosphodiesterase (25).

Drugs acting on pathogen targets that are not present in the host should not cause significant side effects. However, before the human genome was available, the process of identifying bacterial pathogen-specific drug targets was labor intensive, involving comparison of candidate pathogen targets against all known eukaryotic sequences to filter out targets likely to occur in the human (9). Since then, various software tools have made the process of *in silico* target identification in pathogen genomes easier. Available *in silico* tools encompass various cheminformatic (26) and bioinformatic (27, 28) approaches to identify new protein targets. Among the bioinformatic tools, metabolic pathway/metabolic network analysis has emerged as an efficient *in silico* method to identify candidate metabolic enzyme targets in pathogen genomes.

Several software packages are available to facilitate genome-scale metabolic network analyses (29). Starting with an annotated pathogen genome, the components of metabolic pathways are identified, curated and refined (30). The resulting genome-scale metabolic model can be used to integrate omics datasets and to perform various analyses to determine the most likely drug targets (10). Perhaps the most important task with respect to finding good candidate targets is metabolic chokepoint identification. By definition, a chokepoint enzyme either consumes a unique substrate or produces a unique product in the pathogen metabolic network (31).

Inhibition of chokepoint enzymes may disrupt crucial metabolic processes in the pathogen, so chokepoints that are essential to the pathogen represent good potential drug targets (32-34).

The aim of the present study was to characterize the metabolic capabilities of *B. pseudomallei*, identify metabolites and aspects of the metabolic network crucial for pathogen survival, understand the metabolic interactions that occur between pathogen and host cells, and determine if any of the metabolic enzymes produced by the pathogen might be potential antibacterial targets.

This aim was accomplished through genome scale metabolic modeling of *B. pseudomallei* under different external conditions, including all nutrients that could be consumed by the model and only the nutrients available in culture media. Using this approach, we identified candidate chokepoints, then knocked out the genes encoding chokepoint enzymes *in silico* under the different nutrient conditions, and examined the effect of each knockout on the metabolic network. These results demonstrate the utility of genome-scale metabolic modeling methods for *in silico* studies of pathogen metabolism and for drug target identification in *B. pseudomallei*.

Methods

Metabolic pathway reconstructions and annotation curation

Pathway genome databases (PGDBs) for *B. pseudomallei* strains MSHR668 and K96243 were obtained through the Pathway Tools software (version 18.5) from the PGDB registry (35). We found that the original annotation of *B. pseudomallei* K96243 identified many fewer coding sequences than that of MSHR668, so we re-annotated the original complete genome sequences of both strains using the RAST (36) resource to better compare them (37). The RAST-annotated genome sequences were loaded into Pathway Tools, using the PathoLogic component to predict the metabolic pathways (38).

For each genome, the set of protein coding sequences from the original annotation was compared to those from the RAST annotation, using blast to identify coding sequences in common between the two annotations, and to identify coding sequences that were missing from each annotation. For the MSHR668 genome, RAST annotation identified 247 fewer coding sequences than the original annotation. However there were some predicted coding sequences with annotated functions in the RAST annotation that were not present in the original, so these were added to the original PGDB for MSHR668. The RAST annotation of the K96243 genome identified 1,317 more protein coding sequences than the original annotation, so the PGDB that was created from the RAST annotation was used as the starting point. Coding sequences with annotated functions from the original annotation that were not present in the RAST annotation were added to the PGDB that was created from the RAST annotated genome.

Chokepoint Identification

Chokepoints were identified in each PGDB using the chokepoint reaction finder in Pathway Tools. All reactions were included except those found in human.

Flux balance analysis

For each metabolic network reconstruction, flux balance analysis (FBA) was performed using the MetaFlux module within the Pathway Tools (39). Development FBA models were constructed iteratively to determine the compounds that each model could use and produce. This was accomplished by trying all compounds in the PGDB as biomass metabolites, nutrients and secretions in the various compartments (cytosol, periplasmic space and extracellular). Each model was refined iteratively, first identifying the specific biomass components that could be produced, then trying all compounds as nutrients and secretions, then specifying the biomass metabolites and nutrients and trying all compounds as secretions. Once the nutrients, secretions and biomass components that could be consumed or produced by the metabolic networks were determined, the log file produced by MetaFlux was examined and problematic reactions were fixed, if possible. Most of the problematic reactions were unbalanced due to missing chemical formulas of one or more metabolites. A few of these reactions were corrected by copying the missing structures from other PGDBs. For example, the structures of D-ribose, D-glucuronate, D-glucose and some other compounds were copied from the more highly curated *Escherichia coli* K12 substr. MG1655 PGDB. Many of the reactions with compounds that were lacking chemical formulas were generic so no suitable chemical structure could be found or created. For example, reactions involving starch, glycogen, and glucans with variable lengths and non-numeric stoichiometries, could not be balanced. Other reactions were missing H^+ or H_2O on one side or the other, and the addition of these balanced the reaction. However, there were a small number of reactions that could not be fixed and these were marked as unbalanced. Once all reactions that could be fixed were corrected in the PGDB, MetaFlux was run in development mode again to identify additional biomass metabolites, nutrients, and secretions. Once the set of biomass metabolites was constant, the nutrients that could be consumed by the model were determined, and then the secretions. The result of this process was a final unconstrained FBA model utilizing all nutrients that could be consumed by the model.

To mimic the nutrient conditions in culture, only the estimated set of ingredients present in LB medium were included as nutrients in the FBA model. LB medium includes as its main ingredients tryptone (40) and yeast extract (41). Tryptone provides peptides and peptones, which are good sources of amino acids (http://www.sigmaaldrich.com/analytical-chromatography/microbiology/basic-ingredients/protein-sources.html); yeast extract provides vitamins, nitrogenous compounds, carbon, sulfur, trace elements and minerals (42). The LB media composition reported in a *Bacillus subtilis* modeling study (43) was used as a starting point for this study. Starting with the nutrient set that mimicked LB media (43), all compounds were included in the try-biomass set for the cytosol and periplasmic cellular compartments to see which biomass metabolites could be produced given only the nutrients present in LB media. Once a stable set of nutrients was determined, iterations were performed to determine the stable set of biomass metabolites that could be produced. Then all compounds were tried as secretions in the cytosol and periplasmic compartments to determine the compounds that could be secreted by the model.

A list of nutrients that might be available to *B. pseudomallei* while residing inside host cells during infection was compiled by searching the literature for infection studies involving *B. pseudomallei* and host cells. Gene expression studies of other intracellular pathogens and host

cells during infection were also considered. A development FBA model mimicking infection consitions was constructed as described above for the LB media model.

Essential gene and candidate drug target identification

Essential genes in the MSHR668 genome were determined by blasting all protein coding sequences (amino acid format) against the Database of Essential Genes (44) using the blastp program with an E-value cut-off of 1e -10 and 70% identity as thresholds.

Candidate drug target sequences were determined by blasting all protein coding sequences in the MSHR668 genome (as both nucleotide and amino acid formats) against the complete set of DrugBank targets (45), using an E-value cutoff of 0.005 and a threshold identity of 70% to select likely targets.

In silico knockout experiments

To reduce the set of potential drug targets, candidate chokepoint enzymes were compared against the list of essential genes and all of the drug targets in DrugBank to identify chokepoint sequences representing essential genes and DrugBank targets. Knockout experiments were performed *in silico* through the Pathway Tools MetaFlux module (39); the chokepoint genes were knocked out one at a time and the effects on total biomass flux through the metabolic network were noted.

Network visualization

For each PGDB, an .sbml file was exported from the Pathway Tools and loaded into Cytoscape (46) version 3.1.1 for visualization and comparison of network features.

Results

General features of genomes and metabolic networks

The general characteristics of each PGDB and metabolic network for *B. pseudomallei* MSHR668 and K96243 are listed in Table 1.

Table 1. Features of *B. pseudomallei* PGDBs and metabolic networks

Genome (Pathway Tools PGDB)	curated MSHR668 (original + RAST)	curated K96243 (RAST + original)
Coding sequences	7133	7045
Pathways	339	387
Enzymatic reactions	1870	1995
Transport reactions	144	82
Enzymes	1666	1685
Transporters	292	38
Compounds	1397	1578
Metabolic Network		
Nodes (metabolites)	4295	4219
Edges (reaction steps)	10860	9747
Chokepoints		
Producing	444	506
Consuming	419	498

Candidate	479	348
Dead-end reactants	166	217
Dead-end products	72	118

The *B. pseudomallei* MSHR668 and K96243 genomes contained similar numbers of coding sequences, pathways, enzymatic reactions and enzymes. Differences between the PGDBs were noted in the numbers of transporters, transport reactions and compounds. The K96243 PGDB contained fewer transporters and transport reactions and more compounds than MSHR668. In terms of the metabolic network characteristics, both networks contained similar numbers of nodes (representing metabolites), while the MSHR668 network had more edges (reaction steps) than K96243. This is likely due to he more extensive curation of the MSHR668 network that was performed during refinement of the metabolic network models (see Methods).

In a metabolic network, chokepoint reactions either uniquely produce or uniquely consume a metabolite. Inhibiting an enzyme that consumes a unique substrate may cause that metabolite to accumulate, and it may be toxic to the cell; inhibiting an enzyme that produces a unique product may starve the cell of an essential metabolite (31). Identifying chokepoint enzymes in pathogens is a promising *in silico* approach to recognize potential metabolic drug targets. For example, analysis of *Plasmodium falciparum* metabolism revealed that 87.5% of proposed drug targets supported by evidence are chokepoint reactions. However, to be a valid chokepoint, the metabolite in question must be balanced by a producing or consuming reaction and not be a dead-end metabolite (31). Table 1 compares the numbers of chokepoint reactions and dead-end metabolites that were identified in each PGDB. Overall the numbers were similar between the two PGDBs, and the lower numbers of dead-ends in the MSHR668 database were likely due to the more extensive curation performed on the MSHR668 PGDB (see Methods).

Flux balance analysis

Unconstrained FBA model

Given a set of nutrients for consumption, along with secretions and metabolites that can be produced, a FBA model predicts the steady-state flux rates of the metabolic reactions in an organism, and provides an estimate of the overall biomass flux. FBA was conducted on each metabolic network as described in the Methods section. Following several cycles of refinement, an initial unconstrained MSHR668 model was solved. The K96243 development model did not reach a stable solution, likely because there were missing transporter-encoding genes (and possibly other genes) in the PGDB, indicating that the annotation needed more curation. Since the unconstrained MSHR668 model reached a stable solution after performing the initial network curation steps suggested by MetaFlux, only this model was analyzed further.

The FBA model of the unconstrained network in MSHR668, included all possible biomass compounds that could be produced, all nutrients that could be consumed, had no weights imposed on the biomass metabolites and no constraints imposed on the nutrients. [Supplemental material, Final_unconstrained_model_inputs.pdf and Final_unconstrained_model_solution.pdf].

LB media FBA model

To mimic the conditions that *B. pseudomallei* experiences in culture, only the nutrients present in LB media plus glycerol were included in the FBA model (43). Constraints were included on some of the nutrients (ADP, Pi, proton and glycerol). [Supplemental material, Final_LB_model_inputs.pdf and Final_LB_model_solution.pdf].

Table 2. Characteristics of the MSHR668 unconstrained and LB media models

Model	total # rxns	# rxns carrying flux	biomass metabolites produced	nutrients consumed	secre-tions	biomass flux
Unconstrained	3193	1619	1403	667	10	15000.00
LB media	3213	1025	282	47	0	0.079412

In addition to the unconstrained and LB media models, the original plan for this study included the development of a model of *B. pseudomallei* that mimics infection conditions. However, there was very little information available on the growth requirements of *B. pseudomallei* inside human macrophages. Most studies of the nutritional requirements of intracellular pathogens growing inside host cells have been performed on *Legionella pneumophila* (47, 48), which can grow and replicate similarly in human macrophages and amoebae (49). Growing in both human macrophages and amoebae, *L. pneumophila* utilizes amino acids as its main sources of carbon, nitrogen and energy; *L. pneumophila* obtains amino acids from the host through proteasomal degradation (48). However, glucose is also used to feed central metabolism under both culture and infection conditions (50).

Comparing the nutrients provided by the LB media model to the nutrients used by *L. pneumophila* in culture and during infection of amoebae (47), the only difference was the carbohydrate carbon source: glycerol (*B. pseudomallei* LB media (51)) vs. glucose (*L. pneumophila* AYE media (50) and in amoebae (47, 50))

When glycerol was replaced by glucose in the LB media model of *B. pseudomallei*, no FBA solution was found [data not shown]. Several possible explanations for this result are presented in the Discussion.

Host cell infection model

To construct a model representing infection conditions, a list of nutrients present in the host cell cytosol is a required input. However, no comprehensive studies have been performed to identify the complete list of host cell nutrients that are available to *B. pseudomallei* during infection. Also, the specific carbon requirements of *B. pseudomallei* in either human macrophages or amoebae have not been determined. However, a recent study produced whole-genome tiling array expression data to assess *B. pseudomallei* transcriptional responses under 82 different conditions, including infection (52). From their supplemental table S2, a list of metabolic genes expressed in the infection conditions was used to infer the potential nutrients consumed by *B. pseudomallei* during infection. Additional candidate host cell nutrients were identified from the literature, focusing on studies of intracellular pathogen-mammalian host infections. The nutrients identified as potential carbon sources for intracellular survival of various pathogens included

aromatic compounds, such as benzoate and phenylacetic acid and related derivatives (53), sugar acids like gluconate, galactonate, glucuronate, and galacturonate (54), ribo- and deoxyribonucleosides, hexuronates (55), glutathione (56), glucose 6-phosphate (57, 58), glycerol-3-phosphate (59). The complete list of potential host cell nutrients is in the [Supplemental material, Nutrients_infection_model.pdf] file.

When a flux balance analysis was performed using the list of candidate host cell nutrients in a developmental model and trying to identify the biomass metabolites that could be produced, some of the nutrients were not present in any reactions in the MSHR668 PGDB. When the rest of the compounds were included as nutrients in addition to glycerol, none of them were consumed by the model, but glycerol was consumed and biomass was produced. When glycerol was excluded from the nutrient list, none of the other nutrients were consumed and the model was not solvable [data not shown].

Metabolic chokepoints and candidate drug targets

To narrow down the list of metabolic chokepoints, which represented candidate drug targets, essential genes and genes with sequence homology to existing DrugBank targets were identified in the MSHR668 genome. This analysis identified 34 chokepoint genes that were also essential genes and DrugBank targets (Table 3).

Table 3. Chokepoint genes that encode candidate metabolic enzyme drug targets in *B. pseudomallei* MSHR668

locus_tag	Gene symbol	Enzyme name	E.C. number	DrugBank target (drug IDs)	Target in human?	Chokepoint in K96243?	Bp Mutant(s)?
BURPS668_0305	argG^{+}	argininosuccinate synthase	6.3.4.5	P0A6E4 Argininosuccinate synthase (DB00536; DB04077)	no	yes	no*
BURPS668_0328	folB^{+}	dihydroneopterin aldolase	4.1.2.25	P56740 Dihydroneopterin aldolase (DB01778; DB01906; DB02119; DB02489; DB03231; DB03571; DB04168; DB04400; DB04425; DB06906)	no	yes	no
BURPS668_0567	pth^{+}	peptidyl-tRNA hydrolase	3.1.1.29	No	yes	yes	no
BURPS668_0675	aspS^{+}	aspartyl-tRNA synthase	6.1.1.12	P36419 Aspartate--tRNA ligase (DB01895)	no	no	no
BURPS668_0810	RecA^{+}	RecA protein	5.99.1.-	P62219 Protein RecA (DB01660; DB03222; DB04444;	no	yes	no*

				DB04395)			
BURPS668_0964	dut^{+}	deoxyuridine 5'-triphosphate nucleotidohydrolase	3.6.1.19/3.6.1.23	P06968 Deoxyuridine 5'-triphosphate nucleotidohydrolase (DB01965; DB02333; DB03413; DB03800)	no	yes	no
BURPS668_0967	ileS^{+}	isoleucyl-tRNA synthetase	6.1.1.5	Q9NSE4 Isoleucine--tRNA ligase (DB00167)	yes	no	no
BURPS668_1446	pckG^{+}	phosphoenolpyruvate carboxykinase	4.1.1.32	P35558 Phosphoenolpyruvate carboxykinase, cytosolic [GTP] (DB01819; DB02008; DB03267; DB03725)	yes	yes	no
BURPS668_1465	dnaQ^{+}	DNA polymerase III subunit epsilon	2.7.7.7	P03007 DNA polymerase III subunit epsilon (DB01643)	no	yes	no
BURPS668_1544	NA^{+}	alpha-glucosidase	3.2.1.20	O33830 Alpha-glucosidase (DG01769; DB03323)	yes lysosomal	no	no
BURPS668_1669	valS^{+}	valyl-tRNA synthetase	6.1.1.9	P26640 Valine--tRNA ligase (DB00161)	yes	no	no
BURPS668_1712	thrS^{+}	threonyl-tRNA synthetase	6.1.1.3	P0A8M5 Threonine--tRNA ligase (DB03355; DB03869; DB04024)	no	no	no
BURPS668_1750	sucA^{+}	2-oxoglutarate dehydrogenase E1	1.2.4.2	Q02218 2-oxoglutarate dehydrogenase, mitochondrial (DB00157; DB00313)	yes	yes	no
BURPS668_1752	lpdA^{+}	dihydrolipoamide dehydrogenase	1.8.1.4	P14218 Dihydrolipoyl dehydrogenase (DB03147)	no	yes	no
BURPS668_2178	purA^{+}	adenylosuccinate synthetase	6.3.4.4	Q83P33 Adenylosuccinate synthetase (DB02954; DB04160; DB04566)	no	yes	no
BURPS668_2189	hisS^{+}	histidyl-tRNA synthetase	6.1.1.21	P60906 Histidine--tRNA ligase (DB03811; DB04201)	no	no	no
BURPS668_2308	pgi^{+}	glucose-6-phosphate isomerase	5.3.1.9	P06744 Glucose-6-phosphate isomerase (DB02007; DB02076;	yes	no	no

				DB02093; DB02548; DB03042; DB03581; DB03937; DB04493)			
BURPS668_2426	lpxD^{+}	UDP-3-O-[3-hydroxymyristoyl] glucosamine N-acyltransferase	2.3.1.191	O67648 UDP-3-O-[3-hydroxymyristoyl] N-acetylglucosamine deacetylase (DB01991; DB04257; DB04399; DB07355; DB07536; DB08231; DB07861)	no	yes	no
BURPS668_2433	uppS^{+}	undecaprenyl diphosphate synthase	2.5.1.31	P60472 Ditrans,polycis-undecaprenyl-diphosphate synthase ((2E,6E)-farnesyl-diphosphate specific) (DB04695; DB04714; DB07404; DB07409; DB07410; DB07426; DB07780)	no	yes	no
BURPS668_2610	lpdA^{+}	pyruvate dehydrogenase complex E3 component, dihydrolipoamide dehydrogenase	1.8.1.4	P10802 Dihydrolipoyllysine-residue acetyltransferase component of pyruvate dehydrogenase complex (DB01846; DB01992; DB08120)	no	yes	no
BURPS668_2788	fabF^{+}	3-oxoacyl-ACP synthase	2.3.1.41	Q02054 Actinorhodin polyketide synthase acyl carrier protein (DB08585; DB08586)	no	no	no
BURPS668_3103	rfbA^{+}	glucose-1-phosphate thymidylyltransferase	2.7.7.24	Q9HU22 Glucose-1-phosphate thymidylyltransferase (DB01643; DB02452; DB02843; DB03723; DB03751; DB04272; DB04485;	no	yes	no

				DB02452; DB04355)			
BURPS668_3328	tgt^{+}	queuine tRNA-ribosyltransferase	2.4.2.29	P28720 Queuine tRNA-ribosyltransferase (DB01825; DB02041; DB02441; DB02599; DB03074; DB03304; DB03505; DB03780; DB04004; DB04169; DB04239; DB04543; DB07012; DB07452; DB07481; DB07564; DB07704; DB08267; DB08268; DB08511; DB08512; DB08514)	no	yes	no
BURPS668_3366	ruvB^{+}	Holliday junction DNA helicase RuvB	3.1.22.4	Q5SL87 Holliday junction ATP-dependent DNA helicase RuvB (DB00173)	no	no	no
BURPS668_3464	aroQ^{+}	3-dehydroquinate dehydratase	4.2.1.10	P15474 3-dehydroquinate dehydratase (DB02786; DB02801; DB04347; DB04656; DB08485)	no	yes	no
BURPS668_3525	murG^{+}	undecaprenyldiphospho-muramoylpentapeptide beta-N-acetylglucosaminyltransferase	2.4.1.227	P17443 UDP-N-acetylglucosamine--N-acetylmuramyl-(pentapeptide)pyrophosphoryl-undecaprenol N-acetylglucosamine transferase (DB02196)	no	yes	no
BURPS668_3561	ung^{+}	uracil-DNA glycosylase	3.2.2.27	Q8X444 Uracil-DNA glycosylase (DB03419)	no	yes	no
BURPS668_3668	murA^{+}	UDP-N-acetylglucosamine 1-carboxyvinyltransferase		P33038 UDP-N-acetylglucosamine 1-carboxyvinyltransferase (DB01879; DB02435; DB02995; DB03089; DB04174; DB04474)	no	yes	no

BURPS668_A0384	acnD+	aconitate hydratase	4.2.1.3	Q99798 Aconitate hydratase, mitochondrial (DB01727; DB03964; DB04072; DB04351; DB04562); P36683 Aconitate hydratase 2 (DB04351)	yes	yes	no
BURPS668_A1869	ileS+	isoleucyl-tRNA synthetase	6.1.1.5	P41972 isoleucyl-tRNA synthetase (DB00410)	no	no	no
BURPS668_A2053	NA+	putative acetyl-CoA carboxylase, biotin carboxylase	6.3.4.14	P24182 Biotin carboxylase (DB08074; DB08075; DB08076; DB08144; DB08145; DB08146; DB08314; DB08315; DB08316; DB08317; DB08318)	no	yes	no
BURPS668_A2451	leuB+	3-isopropylmalate dehydrogenase	1.1.1.85	Q56268 3-isopropylmalate dehydrogenase (DB04279)	no	yes	no
BURPS668_A2546	polA+	DNA polymerase I	2.7.7.7	P00582 DNA polymerase I (DB00548; DB08432)	no	yes	no
BURPS668_A3190	lpdA+	dihydrolipoamide dehydrogenase	1.8.1.4	P09063 Dihydrolipoyl dehydrogenase (DB03147)	no	yes	no

* mutants exist in other *Burkholderia* species, +essential gene in *B. pseudomallei* K96243 and MSHR668

Eight of the targets in Table 3 were also DrugBank targets in human, so the remaining twenty-six targets were searched in DrugBank, which revealed that they also occur in other bacteria.

In silico knockout experiments were performed with the MetaFlux module of Pathway Tools to test the effect of inhibiting each chokepoint enzyme on *B. pseudomallei* growth under different conditions. These experiments were performed in both the unconstrained and LB media models. Results (Table 4) show that knockout of BURPS668_3328 (*tgt*) and BURPS668_A2451 (*leuB*), eliminated the biomass flux in the unconstrained model, while knockout of BURPS668_2426 (*lpxD*), BURPS668_2433 (*uppS*), and BURPS668_3525 (*murG*) eliminated the biomass flux in the LB media model. Knockout of BURPS668_2433 (*uppS*), and BURPS668_3525 (*murG*) decreased the biomass flux in the unconstrained model, but did not eliminate it.

Table 4. Results of *in silico* knockout experiments on twenty-six chokepoint reactions in *B. pseudomallei*

locus_tag	Gene name	Reaction(s)	Biomass flux (unconstrained model)	Biomass flux (LB media model)
BURPS668_0305	argG	ARGSUCCINSYN-RXN	15000.000000	0.079412
BURPS668_0328	folB	H2NEOPTERINALDOL-RXN	15000.000000	0.079412
BURPS668_0675	aspS	ASPARTATE--TRNA-LIGASE-RXN-ASP-tRNAs/L-ASPARTATE/ATP/PROTON//Charged-ASP-tRNAs/AMP/PPI.60	15000.000000	0.079412
BURPS668_0810	recA	RXN0-5100	15000.000000	0.079412
BURPS668_0964	dut	DUTP-PYROP-RXN	15000.000000	0.079412
BURPS668_1465	dnaQ	DNA-DIRECTED-DNA-POLYMERASE-RXN	15000.000000	0.079412
BURPS668_1712	thrS	THREONINE--TRNA-LIGASE-RXN-THR-tRNAs/THR/ATP/PROTON//Charged-THR-tRNAs/AMP/PPI.52	15000.000000	0.079412
BURPS668_1752	lpdA	RXN-9718	15000.000000	0.079412
BURPS668_2178	purA	ADENYLOSUCCINATE-SYNTHASE-RXN	15000.000000	0.079412
BURPS668_2189	hisS	HISTIDINE--TRNA-LIGASE-RXN-HIS-tRNAs/HIS/ATP/PROTON//Charged-HIS-tRNAs/AMP/PPI.52	15000.000000	0.079412
BURPS668_2426	lpxD	UDPHYDROXYMYRGLUCOSAMNACETYLTRANS-RXN-R-3-hydroxymyristoyl-ACPs/UDP-OHMYR-GLUCOSAMINE//OH-MYRISTOYL/ACP/PROTON.73	15000.000000	0.000000
BURPS668_2433	uppS	RXN-8999	14545.454545	0.000000
BURPS668_2610	lpdA	1.8.1.4-RXN	15000.000000	0.079412
BURPS668_2788	fabF	3-OXOACYL-ACP-SYNTH-RXN /3-OXOACYL-ACP-SYNTH-BASE-RXN /2.3.1.41-RXN / many other reactions	15000.000000	0.079412
BURPS668_3103	rfbA	DTDPGLUCOSEPP-RXN	15000.000000	0.079412
BURPS668_3328	tgt	QUEUOSINE-TRNA-RIBOSYLTRANSFERASE-RXN; RXN0-1321	0.000000	0.079412
BURPS668_3366	ruvB	3.1.22.4-RXN	15000.000000	0.079412
BURPS668_3464	aroQ	3-DEHYDROQUINATE-DEHYDRATASE-RXN	15000.000000	0.079412
BURPS668_3525	murG	RXN-11346, RXN-8976, NACGLCTRANS-RXN, RXN-11029	10000.000000	0.000000
BURPS668_3561	ung	RXN0-2584	15000.000000	0.079412
BURPS668_3668	murA	UDPNACETYLGLUCOSAMENOLPYRTRANS-RXN	15000.000000	0.079412

BURPS668_A1869	ileS	ISOLEUCINE--TRNA-LIGASE-RXN	15000.000000	0.079412
BURPS668_A2053	acc	BIOTIN-CARBOXYL-RXN	15000.000000	0.079412
BURPS668_A2451	leuB	RXN-13158; 3-ISOPROPYLMALDEHYDROG-RXN	0.000000	0.079412
BURPS668_A2546	polA	DNA-DIRECTED-DNA-POLYMERASE-RXN	15000.000000	0.079412
BURPS668_A3190	lpdA	1.8.1.4-RXN/RXN0-1132/RXN-8629	15000.000000	0.079412

The overall biomass fluxes were different in the two models. The unconstrained model had a much greater total biomass flux than the LB media model.

Discussion

Inside host cells, pathogenic bacteria must acquire nutrients to survive, grow and reproduce. Intracellular bacteria are heterotrophic, so they require various sources of carbon, such as carbohydrates, lipids, glycolipids, dicarboxylic acids and amino acids, from their host environment (59, 60). Preferred carbon sources vary among intracellular pathogens, and the types of nutrients available in the host cell cytosol may determine the cell-type specificities of different intracellular pathogens (61). Obviously and unsurprisingly, without adequate nutrition, intracellular pathogens cannot cause disease (62).

It has been suggested that bacterial pathogens survive in the host cell cytosol because they have adapted metabolically to maximize their ability to utilize the available nutrients and grow in that niche (59, 63-65). For example, many bacteria prefer hexoses, like glucose, for carbon and energy sources. These sugars are catabolized through glycolysis, the pentose phosphate and Entner-Doudoroff pathways (60). Some bacteria with different lifestyles lack the glycolysis pathway and preferentially metabolize glucose via the Entner-Doudoroff pathway (66), and some intracellular bacteria lack both glycolysis and Entner-Doudoroff pathways and live on pyruvate that they obtain from the host cell cytosol (67). This diversity in the metabolic capabilities of intracellular pathogens is a fascinating topic, especially because metabolic pathways in the host and pathogen are important to virulence and disease processes. In order to colonize the host, proliferate, establish an infection, and spread to new hosts, pathogens employ various virulence and survival strategies, often involving links between metabolic pathways and virulence genes. Although current knowledge regarding the links between metabolism and virulence is limited (65), this topic is becoming an increasing focus for host-pathogen studies. Some of the general links between metabolism and virulence include regulatory connections between specific metabolites and virulence gene expression (68-72), metabolic requirements for adaptation of the pathogen to the host niche (59, 63-65), and carbon catabolite repression (73). More detailed information on the topic of metabolism and virulence can be found in these recent reviews (59, 62-65, 74-76).

Regardless of the specific metabolic capabilities possessed by a pathogen, essential nutrient acquisition and utilization mechanisms are proving to be good potential therapeutic targets, as

inhibition of these targets would deprive the pathogen of needed substrates for growth and replication inside host cells.

We previously reported that *B. pseudomallei* MSHR668, K96243 and 1106a have abundant capabilities to metabolize hexoses, including the complete sets of genes encoding the glycolysis, pentose phosphate cycle, and Entner-Doudoroff pathways. They also have several pathways for metabolism of pyruvate to acetyl-CoA, acetate and ethanol (37). In general, *B. pseudomallei* as a species has a very diverse set of metabolic capabilities, likely a reflection of its ability to live both in the natural environment and in hosts.

The metabolic power of *B. pseudomallei* has been targeted in mutation studies. Mutation of various metabolic genes results in attenuation of *B. pseudomallei* virulence; these genes include phosphoribosylformylglycinamidine cyclo-ligase (*purM*) (77), aspartate-β-semialdehyde dehydrogenase (*asd*) (78), acetolactate synthase (*ilvI*) (21), dehydroquinate synthase (*aroB*) (20), chorismate synthase (*aroC*) (17), phosphoserine aminotransferase (*serC*) (79), phosphoribosylglycinamide formyltransferase 1 (*purN*) and phosphoribosylformylglycinamide cyclo-ligase (*purM*) (18), two phospholipase C enzymes (80), disulfide oxidoreductase (*dsbA*) (81).

Targeted mutation of *purM*, which encodes aminoimidazole ribotide, a precursor of de novo adenine and thiamine biosynthesis, predictably causes a deficiency in adenine and thiamine biosynthesis (77). Aspartate-β-semialdehyde dehydrogenase (*asd)* mutants cannot synthesize diaminopimelate for cell wall biosynthesis (78), while acetolactate synthase (*ilvI)* mutants cannot synthesize the branched chain amino acids isoleucine, valine, and leucine (21). Dehydroquinate synthase (*aroB)* mutants are defective in the shikimate pathway for chorismate biosynthesis, and addition of the aromatic compounds tyrosine, tryptophan, phenylalanine, PABA, and 2,3-dihydroxybenzoate is required to restore the growth in minimal medium (20). Chorismate synthase (*aroC)* mutants are also defective in aromatic compound synthesis and cannot grow without the addition of aromatic compounds to the media (17). Phosphoserine aminotransferase (*serC*) mutants are defective in serine and pyridoxal 5-phosphate biosynthesis and require minimal medium supplemented with serine for normal growth (79).

Using live attenuated bacteria as vaccines can be effective in preventing disease, as attenuated bacteria may replicate in the host and contain immune-stimulatory epitopes that are not found in subunit or heat-inactivated vaccines (82). Many of the *B. pseudomallei* mutants described above have already been tried as attenuated vaccines with mixed results. Vaccination with the attenuated *asd* mutant protected BALB/c mice against acute melioidosis, but did not protect against chronic melioidosis (78). Vaccination with the attenuated *ilvI* mutant of B. pseudomallei protected BALB/c mice against a challenge with a virulent strain (21). In mice vaccinated with the *aroB* mutant, the time to death following challenge with the virulent K96243 strain was a bit longer than in unvaccinated mice, but all mice eventually died (20). The *aroC* mutant was unable to persist in vaccinated BALB/c mice long enough to elicit protective immunity, however C57BL/6 mice were protected against challenge with a virulent strain (17). Intraperitoneal vaccination of BALB/c mice with a *serC* mutant resulted in higher levels of survival after challenge with K96243 virulent strain (79).

While immunization of mice with attenuated *B. pseudomallei* mutants has resulted in the induction of protective immunity in some cases, sterile immunity was rarely reported (reviewed by (83)). Also, the live attenuated vaccine model may not be the best solution for the prevention of melioidosis, because an attenuated mutant might revert to virulence, and might also establish a latent infection (83).

An alternative avenue to combat melioidosis is through antimicrobial therapeutics. With genomic sequencing technologies becoming more affordable, to date there are 393 *B. pseudomallei* genomes available at the National Center for Biotechnology Information (NCBI, http://www.ncbi.nlm.nih.gov/genome/476). While some of these entries represent re-annotations of previous submissions, and there are some genomes representing colony morphology variants of the same strain, an impressive number of individual genomes are available to use with computational approaches to identify new therapeutic targets.

In silico methods for the identification of therapeutic targets in bacterial pathogens include comparative genomics-based approaches, such as identification of essential genes specific to the pathogen, and techniques based on metabolic pathway analysis and metabolic network modeling. The more robust approaches use a combination of comparative genomics methods and metabolic pathway analysis. Two studies computationally identified essential gene targets in genomes of the bacterial pathogens *Mycoplasma genitalium* (84) and *Mycobacterium ulcerans* (85). Another method, subtractive target identification, involves identification of enzymes in the metabolic pathways of the pathogen, and comparing them to human proteins to identify pathogen enzymes that are not found in human. A list of likely targets is compiled by focusing on enzymes in pathways that are usually essential for pathogen growth and survival, like lipid metabolism, carbohydrate metabolism, amino acid metabolism, energy metabolism, vitamin and cofactor biosynthetic pathways and nucleotide metabolism. This approach has been used to identify putative targets in *M. tuberculosis* (86), MRSA (87-89) and a collection of other bacterial pathogens (90).

Methods for therapeutic target discovery based on metabolic pathway analysis and metabolic network modeling have become very popular in the last ten years. Numerous studies have identified candidate drug targets in various bacterial (27, 34, 91-102), fungal (102) and protosoan (31, 102-105) pathogens using a variety of methods to analyze metabolic pathways and networks. One method employs chokepoint analysis to identify metabolic enzymes that are critical to the pathogen, because they uniquely consume and/or produce certain metabolites. Chokepoint analysis has been used to identify candidate metabolic enzyme targets in various pathogen (27, 31, 34, 95, 103, 104, 106, 107). However, no studies to date have identified potential drug targets using a chokepoint analysis of *B. pseudomallei* metabolic networks.

For this study, a chokepoint analysis was performed on the curated *B. pseudomallei* MSHR668 metabolic network using the Pathway Tools software (35). Table 3 lists the chokepoint enzymes identified in the metabolic networks of *B. pseudomallei* MSHR668 and K96243. Twenty-four of the *B. pseudomallei* chokepoints were not indicated as human targets in DrugBank, and therefore represented good candidate therapeutic targets against melioidosis. Six of the chokepoints in Table 3 were aminoacyl-tRNA synthetases, which are likely good targets as they are critical enzymes involved in protein translation. These chokepoints included aspartyl-, threonyl-,

histidyl-, valyl- and isoleucyl-tRNA synthetase (2 copies). **A**spartyl-tRNA synthase (*aspS*) is an essential gene target in *M. tuberculosis* (108). Threonyl-tRNA synthetase (*thrS*) inhibitors have been identified (109) and shown to have anti-malarial activity against *Plasmodium falciparum* (110). Isoleucyl-tRNA synthetase (*ileS*) is a well-documented bacterial target (111-113). The antimicrobial drug, mupirocin (pseudomonic acid), selectively inhibits bacterial isoleucyl-tRNA synthetase without inhibiting its human homolog (110). However, resistance is seen in bacteria that possess an isoleucyl-tRNA synthetase that is similar to eukaryotic versions (114). Histidyl-tRNA synthetase (*hisS*) has been explored as a target in *Trypanosoma cruzi* (115). The chokepoint enzyme queuine tRNA-ribosyltransferase (*tgt*) incorporates the wobble base queuine into tRNA, and is also a target in *Zymomonas mobilis* and *Shigella* (116, 117)

Several *B. pseudomallei* chokepoint enzymes are involved in DNA-related processes. Two of these enzymes, encoded by the *recA* and *dnaQ* genes, are involved in the SOS pathway (118), which mediates the bacterial response to DNA damage. Activation of the SOS response by ciprofloxacin induces mutations, which can lead to fluoriquinolone resistance (119). The RecA protein is a target for antibacterial drug discovery in *M. tuberculosis* (120) and *Mycoplasma hyopneumoniae* (92), and has been proposed as a specific target for reducing the evolution of antimicrobial resistance (121). The chokepoint enzyme deoxyuridine 5'-triphosphate nucleotidohydrolase (dUTPase) prevents incorporation of uracil into DNA and is important for DNA integrity (122). dUTPase is a potential antimalarial drug target against *P. falciparum* (123, 124). Holliday junction DNA helicase (*ruvB*) participates in homologous recombination and repair of replication forks, and is therefore essential for bacterial growth. Holliday junction processing components were previously identified as targets for antimicrobials in *E. coli* (125) and *Neisseria gonorrhoeae* (126). The chokepoint enzyme uracil-DNA glycosylase (*ung*) has a role in uracil excision repair, and is a candidate anti-malarial drug target (127), as well as a potential target to control growth of GC-rich bacteria such as *Pseudomonas aeruginosa* and *Mycobacterium smegmatis* (128). DNA polymerase I was identified as a chokepoint in *B. pseudomallei*. Putative inhibitors of DNA polymerase I (*polA*), and subsequently DNA synthesis, have been explored as possible antimicrobials (129, 130).

Some chokepoint enzymes in *B. pseudomallei* have functions in the biosynthesis of cell wall components. One of these chokepoints, UDP-3-O-[3-hydroxymyristoyl] glucosamine N-acyltransferase (*lpxD*), catalyzes the third step in the lipid A biosynthesis pathway (131). The lipid A component of bacterial LPS is of particular interest because it is essential for cell viability and is highly conserved (132). This pathway is a target for new antibacterial therapeutics in *Escherichia coli* (133). Another chokepoint involved in cell wall synthesis is undecaprenyl diphosphate synthase (*uppS*), which catalyzes the synthesis of a polyisoprenoid essential for both peptidoglycan and cell wall teichoic acid synthesis. UppS is a critical enzyme required for bacterial survival, and is an antibacterial target in *Staphylococcus aureus* (134), *Bacteroides fragilis*, *Vibrio vulnificus*, *E. coli* (135) and *H. pylori* (136). Several classes of compounds that inhibit UppS function have been discovered (134, 137, 138). Two additional *B. pseudomallei* chokepoints, undecaprenyldiphospho-muramoylpentapeptide beta-N-acetylglucosaminyltransferase (*murG*), and UDP-N-acetylglucosamine 1-carboxyvinyltransferase (*murA*) are involved in peptidoglycan biosynthesis. MurG is the target of the antibiotic ramoplanin in *Staphylococcus aureus* (139). Other potential inhibitors of MurG have been identified by high throughput screening (140). A small molecule inhibitor of MurG

that augments the activity of β-lactams against methicillin-resistant *Staphylococcus aureus* was recently identified (141). MurA has been a popular target for the design of novel antibiotics, and several inhibitors of MurA have been identified that are active against various bacterial species (87, 142-147). The chokepoint enzyme glucose-1-phosphate thymidylyltransferase (*rfbA/rmlA*), involved in O antigen biosynthesis, is also a target in *Streptococcus pneumoniae* (148) and *Pseudomonas aeruginosa* (149).

The rest of the chokepoint enzymes in Table 3 were components of various biosynthesis pathways. These enzymes included argininosuccinate synthase (*argG*), which catalyzes the second to last step in L-arginine biosynthesis, and is associated with pathogenesis in the parasite *Leishmania donovani* (150), *Streptococcus pneumoniae* (151), and *B. cenocepacia* (152). The chokepoint enzyme 3-isopropylmalate dehydrogenase (*leuB*) is the third enzyme specific to leucine biosynthesis in microorganisms (153), and has been investigated as an antibacterial target in *M. tuberculosis* (154). The *B. pseudomallei* chokepoint dihydroneopterin aldolase (*folB*) is part of the tetrahydrofolate biosynthesis process, and is essential for growth and biomass production in *Acinetobacter baylyi*, *Bacillus anthracis*, *Francisella tularensis*, *F. tularensis* subsp. novicida strain U112, *Mycobacterium tuberculosis*, *Helicobacter pylori*, *Pseudomonas aeruginosa*, *Salmonella enterica* serovar Typhi and *Yersinia pestis* (91). Three of the chokepoint genes identified in *B. pseudomallei* encoded lipoamide dehydrogenase, a component of the pyruvate dehydrogenase complex, which converts pyruvate to acetyl-CoA as part of central metabolism (155). Lipoamide dehydrogenase is also a target in *M. tuberculosis*, where deletion drastically impaired the pathogen's ability to establish infection in the mouse (156). The mycobacterial version has only 36% identity with the human homolog. Lipoamide dehydrogenase is a target of drugs against trypanosomal infections (157). Adenylosuccinate synthetase (*purA*) is also a chokepoint enzyme and potential therapeutic target that is involved in purine salvage in *Leishmania donovani* (158). Chokepoint enzyme 3-dehydroquinate dehydratase (*aroQ*) is a component of the shikimate pathway for chorismate biosynthesis and is a target of known inhibitors in *M. tuberculosis*, *Enterococcus faecalis* and *Streptomyces coelicolor* (159-163).

The *B. pseudomallei* chokepoint enzyme 3-oxoacyl-ACP synthase (*fabF*), involved in fatty acid synthesis, is already an antibacterial target in *E. coli*, and a specific inhibitor, cerulenin, has been identified (164, 165). Another fatty acid synthesis chokepoint enzyme in *B. pseudomallei* was a biotin-dependent acetyl-CoA carbosylase. Biotin dependent carboxylases comprise a large group of enzymes that participate in a variety of cellular processes, including fatty acid metabolism, amino acid metabolism, carbohydrate metabolism, polyketide biosynthesis, urea utilization, etc. (reviewed by (166)). Acetyl-CoA carboxylase is comprised of two enzymes, biotin carboxylase and carboxyltransferase, and catalyzes the first committed step in fatty acid synthesis (167). Acetyl-CoA carboxylase is an antimicrobial target in *M. tuberculosis* (168), *E. coli* (169, 170), other bacteria and most living organisms (reviewed by (171)). All of the chokepoints in Table 3 are essential genes in *B. pseudomallei* MSHR668 and K96243, as determined by blasting the chokepoint enzyme sequences against essential gene sequences in the Database of Essential Genes (172) and by comparing to the list of essential genes previously identified in K96243 (173).

To determine if *B. pseudomallei* deletion mutants were available for each of the chokepoints in

Table 3, searches of the internet, PubMed, and the Burkholderia Genome Database (http://burkholderia.com) were performed. Based on these searches, none of the chokepoint enzymes in Table 3 had a mutant available; however, a *B. cenocepacia argG* mutant has attenuated virulence (174), and *recA* mutants have been identified in *B. cepacia* (175).

Additional metabolic enzymes, not identified as chokepoints in this study, and pathways critical for bacterial growth and survival have been called out previously with respect to target identification. These include anaplerotic pathways that turned on by limiting carbon sources (176), the glyxoalate shunt enzyme isocitrate lyase (16, 177, 178), involved in the metabolism of fatty acids (15, 177), enoyl-ACP reductase (FabI) in the type II fatty acid biosynthesis pathway (179), and alanine racemase (23).

To gain an understanding of the metabolic processes in *B. pseudomallei* MSHR668 that are active under different environmental conditions, and to test the effect of deletion of each chokepoint enzyme on the growth of *B. pseudomallei in silico*, metabolic network models were constructed and FBA was performed. The first FBA model, of the unconstrained network in MSHR668, included all possible biomass compounds that could be produced, all nutrients that could be consumed, had no weights imposed on the biomass metabolites and no constraints imposed on the nutrients. [Supplemental material, Final_unconstrained_model_inputs.pdf and Final_unconstrained_model_solution.pdf]. This model likely represents the metabolic potential of B. pseudomallei in a soil or water environment where abundant carbon and nitrogen sources are available. To mimic the conditions that *B. pseudomallei* experiences in culture, a separate model was constructed that provided only the nutrients present in LB media plus glycerol (43). Constraints were included on some of the nutrients in this model (ADP, Pi, proton and glycerol). [Supplemental material, Final_LB_model_inputs.pdf and Final_LB_model_solution.pdf].

A third model was attempted, to mimic infection conditions using only the nutrients present in the host cell cytosol. However, no comprehensive studies have identified a complete list of host cell nutrients that are available to *B. pseudomallei* during infection. Also, the specific carbon requirements of *B. pseudomallei* in either human macrophages or amoebae have not been determined. After trying to compile a list of nutrients that mimic the content of the host cytosol, from the literature and from gene expression studies of B. pseudomallei during infection, this model did not produce a solution so it was abandoned. However, the LB media model contained a similar set of nutrients, so it may in fact be somewhat representative of infection conditions.

In terms of carbon sources, glucose was utilized as a nutrient in the unconstrained model of MSHR668. However, when glycerol was replaced by glucose in the LB media model, no FBA solution was found [data not shown]. This was a somewhat unexpected result, as *B. pseudomallei* can utilize glucose as a carbon source in culture (180). One possible explanation for this result is that additional nutrients required for glucose utilization were missing from the input nutrients list. Co-metabolism of more than one carbon substrate is a metabolic strategy employed by intracellular bacteria replicating inside host cells to provide carbon for energy and biosynthesis (59). For example, *Listeria monocytogenes* can use both glycerol and lactate as carbon sources, (57, 181-183). It has been suggested that during infection by *Listeria*, the host cell may not contain enough glucose to activate bacterial PTS glucose transporters, so alternative carbon sources are important for survival and virulence of the pathogen (57). *M. tuberculosis* also relies

on glycerol and fatty acids as carbon sources in the macrophage environment (184) As the unconstrained *B. pseudomallei* model included a much longer list of nutrients than the LB model and also could use glucose as a nutrient, this could be the case. Another explanation for glucose not being utilized by the LB media model is that intracellular bacteria seem to prefer other substrates over glucose during infection (185), and glycerol may be a major carbon source for intracellular bacteria during infection (185, 186). This may also be the situation for *B. pseudomallei* inside host cells. Glycerol feeds into the second half of the glycolysis/gluconeogenesis pathway through its conversion to dihydroxyacetone phosphate [www.metacyc.org; (187)], bypassing the first four steps of glycolysis. We previously determined that the *B. pseudomallei* MSHR668 genome has the full set of genes to perform this conversion (37). Two studies of *Listeria monocytogenes* infection support the idea that intracellular pathogens generally may use glycerol rather than glucose as a main carbon source while inside host cells. Transcription profiles of *L. monocytogenes* grown in mouse macrophages showed reduced expression of genes encoding some of the enzymes involved in glycolysis, in particular phosphoglucose isomerase (*pgi*), which converts glucose-6-phosphate into fructose-6-phosphate, and the five steps involved in the conversion of glyceraldehyde-3-phosphate to pyruvate (185). Similar transcription profiles were seen during *L. monocytogenes* infection of Caco-2 epithelial cells (188). Both studies showed increased expression of genes involved in the uptake and utilization of glycerol (185, 188): these genes were *glpF*, *glpK*, *glpD* and *dhaK*.

To date, no study has determined precisely which carbon substrates are utilized by *B. pseudomallei* during infection of macrophages. In addition to glycerol, there is evidence that *B. pseudomallei* may utilize aromatic carbon compounds such as benzoate and phenylacetic acid as carbon sources for intracellular survival (53). One study showed that in *B. pseudomallei* 1026b, glycolytic pathway and TCA cycle genes were down-regulated during infection of hamster (189), supporting the idea that *B. pseudomallei* may prefer carbon sources other than glucose while inside host cells. Other studies examined genes induced by hypoxia, which is a condition present in infected macrophages (190) and changes in *B. pseudomallei* gene expression during infection of rat lungs (191), but these only provide further clues about *B. pseudomallei*'s carbon preferences during infection.

Complicating the situation even more, the complete nutrient content of a representative mammalian host cell cytosol has not been determined yet, so we are even farther from identifying a consensus set of nutrients present in the cytosol of different host cell types (186). This is largely due to the challenges in designing appropriate infection models and identifying robust analytical approaches to measure metabolic changes occurring in host cells during infection. Because of these limitations on both the pathogen and host sides, it is difficult to predict which carbon sources pathogens can use to grow inside host cells.

While we don't know the exact biochemical composition of a mammalian cell cytosol, we do know some details about mammalian cells in general. For example, the cytosol of a typical cell has low magnesium, sodium and calcium concentrations, and a high potassium concentration at neutral pH (192). In addition, mammalian cells contain small amounts of amino acids, plus significant amounts of TCA cycle intermediates (193, 194). Once inside host cells, intracellular bacteria may stimulate host cell responses to produce needed nutrients (186). However, host-pathogen interactions during infection are complicated, as some host defense responses are aimed at inhibiting pathogen survival and proliferation, for instance by decreasing metabolic

activities that provide nutrients to the pathogen (176).

This work is the first to use genome scale metabolic modeling to address *B. pseudomallei* metabolism as a source of new drug targets. While identifying the nutrients available to *B. pseudomallei* inside host cells was difficult, the effort described here identified a set of 26 chokepoint enzyme drug targets; *in silico* deletion of 4 of these target enzymes reduced the total biomass flux through the *B. pseudomallei* metabolic network. While this genome-based approach can streamline the initial steps of antibacterial target identification, the true utility of this process will be demonstrated when the targets are experimentally verified by performing knockout experiments in culture, followed by efficacy testing of candidate drugs in culture and in animal models of infection.

Acknowledgements
This project was funded by the Defense Threat Reduction Agency

References

1. **White NJ.** 2003. Melioidosis. Lancet **361:**1715-1722.
2. **Currie BJ.** 2003. Melioidosis: an important cause of pneumonia in residents of and travellers returned from endemic regions. Eur Respir J **22:**542-550.
3. **Schweizer HP.** 2012. Mechanisms of antibiotic resistance in *Burkholderia pseudomallei*: implications for treatment of melioidosis. Future Microbiol. **7:**1389-1399.
4. **Dance D.** 2014. Treatment and prophylaxis of melioidosis. Int J Antimicrob Agents. **43:**310-318.
5. **Mays EE, Ricketts EA.** 1975. Melioidosis: recrudescence associated with bronchogenic carcinoma twenty-six years following initial geographic exposure. Chest **68**.
6. **Thibault FM, Hernandez E, Vidal DR, Girardet M, Cavallo JD.** 2004. Antibiotic susceptibility of 65 isolates of *Burkholderia pseudomallei* and *Burkholderia mallei* to 35 antimicrobial agents. J. Antimicrob. Chemother. **54:**1134-1138.
7. **Jenney AW, Lum G, Fisher DA, Currie BJ.** 2001. Antibiotic susceptibility of *Burkholderia pseudomallei* from tropical northern Australia and implications for therapy of melioidosis. Int. J. Antimicrob. Agents **17:**109-113.
8. **Dance DA, Wuthiekanun V, Chaowagul W, White NJ.** 1989. The antimicrobial susceptibility of *Pseudomonas pseudomallei*. Emergence of resistance in vitro and during treatment. J Antimicrob Chemother. **24:**295-309.
9. **Galperin MY, Koonin EV.** 1999. Searching for drug targets in microbial genomes. Curr Opin Biotechnol. **10:**571-578.
10. **Oberhardt MA, Yizhak K, Ruppin E.** 2013. Metabolically re-modeling the drug pipeline. Curr Opin Pharmacol. **13:**778-785.
11. **Silver LL.** 2011. Challenges of antibacterial discovery. Clin Microbiol Rev. **24:**71-109.
12. **Cummings JE, Kingry LC, Rholl DA, Schweizer HP, Tonge PJ, Slayden RA.** 2014. The *Burkholderia pseudomallei* enoyl-acyl carrier protein reductase FabI1 is essential for in vivo growth and is the target of a novel chemotherapeutic with efficacy. Antimicrob Agents Chemother. **58:**931-935.
13. **Lu H, Tonge PJ.** 2008. Inhibitors of FabI, an enzyme drug target in the bacterial fatty acid biosynthesis pathway. Acc Chem Res. **41:**11-20.

14. **Tong L, Harwood HJJ.** 2006. Acetyl-coenzyme A carboxylases: versatile targets for drug discovery. J Cell Biochem **99:**1478-1488.
15. **Muñoz-Elías EJ, McKinney JD.** 2005. *Mycobacterium tuberculosis* isocitrate lyases 1 and 2 are jointly required for in vivo growth and virulence. Nat Med. **11:**638-644.
16. **van Schaik EJ, Tom M, Woods DE.** 2009. *Burkholderia pseudomallei* isocitrate lyase is a persistence factor in pulmonary melioidosis: implications for the development of isocitrate lyase inhibitors as novel antimicrobials. Infect Immun. **77:**4275-4283.
17. **Srilunchang T, Proungvitaya T, Wongratanacheewin S, Strugnell R, Homchampa P.** 2009. Construction and characterization of an unmarked aroC deletion mutant of *Burkholderia pseudomallei* strain A2. Southeast Asian J Trop Med Public Health **40:**123-130.
18. **Breitbach K, Köhler J, Steinmetz I.** 2008. Induction of protective immunity against *Burkholderia pseudomallei* using attenuated mutants with defects in the intracellular life cycle. Trans R Soc Trop Med Hyg **102 Suppl 1:**S89-94.
19. **Pilatz S, Breitbach K, Hein N, Fehlhaber B, Schulze J, Brenneke B, Eberl L, Steinmetz I.** 2006. Identification of *Burkholderia pseudomallei* genes required for the intracellular life cycle and in vivo virulence. Infect Immun **74:**3576-3586.
20. **Cuccui J, Easton A, Chu KK, Bancroft GJ, Oyston PC, Titball RW, Wren BW.** 2007. Development of signature-tagged mutagenesis in *Burkholderia pseudomallei* to identify genes important in survival and pathogenesis. Infect Immun **75:**1186-1195.
21. **Atkins T, Prior RG, Mack K, Russell P, Nelson M, Oyston PC, Dougan G, Titball RW.** 2002. A mutant of *Burkholderia pseudomallei*, auxotrophic in the branched chain amino acid biosynthetic pathway, is attenuated and protective in a murine model of melioidosis. Infect Immun **70:**5290-5294.
22. **Levine HB, Maurer RL.** 1958. Immunization with an induced avirulent auxotrophic mutant of *Pseudomonas pseudomallei*. J Immunol **81:**433-438.
23. **Zajdowicz SL, Jones-Carson J, Vazquez-Torres A, Jobling MG, Gill RE, Holmes RK.** 2011. Alanine racemase mutants of *Burkholderia pseudomallei* and *Burkholderia mallei* and use of alanine racemase as a non-antibiotic-based selectable marker. PLoS One **6:**e21523.
24. **Vanaporn M, Wand M, Michell SL, Sarkar-Tyson M, Ireland P, Goldman S, Kewcharoenwong C, Rinchai D, Lertmemongkolchai G, Titball RW.** 2011. Superoxide dismutase C is required for intracellular survival and virulence of *Burkholderia pseudomallei*. Microbiology **157:**2392-2400.
25. **Lee HS, Gu F, Ching SM, Lam Y, Chua KL.** 2010. CdpA is a *Burkholderia pseudomallei* cyclic di-GMP phosphodiesterase involved in autoaggregation, flagellum synthesis, motility, biofilm formation, cell invasion, and cytotoxicity. Infect Immun **78:**1832-1840.
26. **McPhillie MJ, Cain RM, Narramore S, Fishwick CW, Simmons KJ.** 2015. Computational methods to identify new antibacterial targets. Chem Biol Drug Des. **85:**22-29.
27. **Chung BK, Dick T, Lee DY.** 2013. In silico analyses for the discovery of tuberculosis drug targets. J Antimicrob Chemother. **68:**2701-2709.
28. **Mobegi FM, van Hijum SA, Burghout P, Bootsma HJ, de Vries SP, van der Gaast-de Jongh CE, Simonetti E, Langereis JD, Hermans PW, de Jonge MI, Zomer A.**

2014. From microbial gene essentiality to novel antimicrobial drug targets. BMC Genomics **15:**958.
29. **Hamilton JJ, Reed JL.** 2014. Software platforms to facilitate reconstructing genome-scale metabolic networks. Environ Microbiol. **16:**49-59.
30. **Thiele I, Palsson BØ.** 2010. A protocol for generating a high-quality genome-scale metabolic reconstruction. Nat. Protoc. **5:**93-121.
31. **Yeh I, Hanekamp T, Tsoka S, Karp PD, Altman RB.** 2004. Computational analysis of *Plasmodium falciparum* metabolism: Organizing genomic information to facilitate drug discovery. Genome Res **14:**917-924.
32. **Duffield M, Cooper I, McAlister E, Bayliss M, Ford D, Oyston P.** 2010. Predicting conserved essential genes in bacteria: in silico identification of putative drug targets. Mol Biosyst. **6:**2482-2489.
33. **Sakharkar KR, Sakharkar MK, Chow VT.** 2004. A novel genomics approach for the identification of drug targets in pathogens, with special reference to *Pseudomonas aeruginosa*. In Silico Biol. **4:**355-360.
34. **Singh S, Malik BK, Sharma DK.** 2007. Metabolic pathway analysis of *S. pneumoniae*: an in silico approach towards drug-design. J Bioinform Comput Biol **5:**135-153.
35. **Karp PD, Paley S, Romero P.** 2002. The Pathway Tools software. Bioinformatics **18 Suppl 1:**S225-S232.
36. **Aziz RK, Bartels D, Best AA, DeJongh M, Disz T, Edwards RA, Formsma K, Gerdes S, Glass EM, Kubal M, Meyer F, Olsen GJ, Olson R, Osterman AL, Overbeek RA, McNeil LK, Paarmann D, Paczian T, Parrello B, Pusch GD, Reich C, Stevens R, Vassieva O, Vonstein V, Wilke A, Zagnitko O.** 2008. The RAST Server: rapid annotations using subsystems technology. BMC Genomics **9:**75.
37. **Challacombe JF, Stubben CJ, Klimko CP, Welkos SL, Kern SJ, Bozue JA, Worsham PL, Cote CK, Wolfe DN.** 2014. Interrogation of the *Burkholderia pseudomallei* genome to address differential virulence among isolates. PLoS One **9:**e115951.
38. **Karp PD, Latendresse M, Caspi R.** 2011. The pathway tools pathway prediction algorithm. Stand Genomic Sci **5:**424-429.
39. **Latendresse M, Krummenacker M, Trupp M, Karp PD.** 2102. Construction and completion of flux balance models from pathway databases. Bioinformatics **28:**388-396.
40. **Fraser D, Powell RE.** 1950. The kinetics of trypsin digestion. J Biol Chem. **187:**803-820.
41. **Bertani G.** 1951. Studies on lysogenesis. I. The mode of phage liberation by lysogenic *Escherichia coli*. J Bacteriol. **62:**293-300.
42. **Grant CL, Pramer D.** 1962. Minor element composition of yeast extract. J Bacteriol. **84:**869-870.
43. **Oh YK, Palsson BO, Park SM, Schilling CH, Mahadevan R.** 2007. Genome-scale reconstruction of metabolic network in *Bacillus subtilis* based on high-throughput phenotyping and gene essentiality data. J Biol Chem. **282:**28791-28799.
44. **Zhang R, Lin Y.** 2009. DEG 5.0, a database of essential genes in both prokaryotes and eukaryotes. Nucleic Acids Res. **37(Database issue):**D455-458.
45. **Wishart DS, Knox C, Guo AC, Cheng D, Shrivastava S, Tzur D, Gautam B, Hassanali M.** 2008. DrugBank: a knowledgebase for drugs, drug actions and drug targets. Nucleic Acids Res. **36(Database issue):**D901-906.

46. **Shannon P, Markiel A, Ozier O, Baliga NS, Wang JT, Ramage D, Amin N, Schwikowski B, Ideker T.** 2003. Cytoscape: a software environment for integrated models of biomolecular interaction networks. Genome Res **13:**2498-2504.
47. **Price CT, Richards AM, Abu Kwaik Y.** 2014. Nutrient generation and retrieval from the host cell cytosol by intra-vacuolar *Legionella pneumophila*. Front Cell Infect Microbiol **4:**111.
48. **Price CT, Abu Kwaik Y.** 2012. Amoebae and mammals deliver protein-rich Atkins diet meals to *Legionella* cells. Microbe **7:**506-513.
49. **Gao LY, Harb OS, Abu Kwaik Y.** 1997. Utilization of similar mechanisms by *Legionella pneumophila* to parasitize two evolutionarily distant host cells, mammalian macrophages and protozoa. Infect. Immun. **65:**4738-4746.
50. **Eylert E, Herrmann V, Jules M, Gillmaier N, Lautner M, Buchrieser C, Eisenreich W, Heuner K.** 2010. Isotopologue profiling of *Legionella pneumophila*: role of serine and glucose as carbon substrates. J Biol Chem. **285:**22232-22243.
51. **DeShazer D.** 2004. Genomic Diversity of *Burkholderia pseudomallei* Clinical Isolates: Subtractive Hybridization Reveals a *Burkholderia mallei*-Specific Prophage in B. pseudomallei 1026b. J. Bacteriol. **186:**3938-3950.
52. **Ooi WF, Ong C, Nandi T, Kreisberg JF, Chua HH, Sun G, Chen Y, Mueller C, Conejero L, Eshaghi M, Ang RM, Liu J, Sobral BW, Korbsrisate S, Gan YH, Titball RW, Bancroft GJ, Valade E, Tan P.** 2013. The condition-dependent transcriptional landscape of *Burkholderia pseudomallei*. PLoS Genet. **9:**e1003795.
53. **Chieng S, Carreto L, Nathan S.** 2012. *Burkholderia pseudomallei* transcriptional adaptation in macrophages. BMC Genomics **13:**328.
54. **Eriksson S, Lucchini S, Thompson A, Rhen M, Hinton JC.** 2003. Unravelling the biology of macrophage infection by gene expression profiling of intracellular *Salmonella enterica*. Mol Microbiol **47:**103-118.
55. **Zdziarski J, Brzuszkiewicz E, Wullt B, Liesegang H, Biran D, Voigt B, Grönberg-Hernandez J, Ragnarsdottir B, Hecker M, Ron EZ, Daniel R, Gottschalk G, Hacker J, Svanborg C, Dobrindt U.** 2010. Host imprints on bacterial genomes--rapid, divergent evolution in individual patients. PLoS Pathog. **6:**e1001078.
56. **Reniere ML, Whiteley AT, Hamilton KL, John SM, Lauer P, Brennan RG, Portnoy DA.** 2015. Glutathione activates virulence gene expression of an intracellular pathogen. Nature **517:**70-31.
57. **Eylert E, Schär J, Mertins S, Stoll R, Bacher A, Goebel W, Eisenreich W.** 2008. Carbon metabolism of *Listeria monocytogenes* growing inside macrophages. Mol Microbiol. **69:**1008-1017.
58. **Chico-Calero I, Suárez M, González-Zorn B, Scortti M, Slaghuis J, Goebel W, Vázquez-Boland JA, Consortium ELG.** 2002. Hpt, a bacterial homolog of the microsomal glucose- 6-phosphate translocase, mediates rapid intracellular proliferation in Listeria. Proc Natl Acad Sci U S A **99:**431-436.
59. **Eisenreich W, Dandekar T, Heesemann J, Goebel W.** 2010. Carbon metabolism of intracellular bacterial pathogens and possible links to virulence. Nat Rev Microbiol **8:**401-412.
60. **Muñoz-Elías EJ, McKinney JD.** 2006. Carbon metabolism of intracellular bacteria. Cell Microbiol. **8:**10-22.

61. **Brown SA, Palmer KL, Whiteley M.** 2008. Revisiting the host as a growth medium. Nat Rev Microbiol. **6:**657-666.
62. **Abu Kwaik Y, Bumann D.** 2013. Microbial quest for food in vivo: 'nutritional virulence' as an emerging paradigm. Cell Microbiol. **15:**882-890.
63. **Ray K, Marteyn B, Sansonetti PJ, Tang CM.** 2009. Life on the inside: the intracellular lifestyle of cytosolic bacteria. Nat Rev Microbiol **7:**333-340.
64. **Rohmer L, Hocquet D, Miller SI.** 2011. Are pathogenic bacteria just looking for food? Metabolism and microbial pathogenesis. Trends Microbiol. **19:**341-348.
65. **Fuchs TM, Eisenreich W, Heesemann J, Goebel W.** 2012. Metabolic adaptation of human pathogenic and related nonpathogenic bacteria to extra- and intracellular habitats. FEMS Microbiol Rev. **36:**435-462.
66. **Fuhrer T, Fischer E, Sauer U.** 2005. Experimental identification and quantification of glucose metabolism in seven bacterial species. J Bacteriol. **187:**1581-1590.
67. **Renesto P, Ogata H, Audic S, Claverie JM, Raoult D.** 2005. Some lessons from *Rickettsia* genomics. FEMS Microbiol Rev **29:**99-117.
68. **Gore AL, Payne SM.** 2010. CsrA and Cra influence *Shigella flexneri* pathogenesis. Infect Immun. **78:**4674-4682.
69. **Litwin CM, Calderwood SB.** 1993. Role of iron in regulation of virulence genes. Clin Microbiol Rev. **6:**137-149.
70. **Mellies JL, Barron AM, Carmona AM.** 2007. Enteropathogenic and enterohemorrhagic *Escherichia coli* virulence gene regulation. Infect Immun **75:**4199-4210.
71. **Njoroge JW, Nguyen Y, Curtis MM, Moreira CG, Sperandio V.** 2012. Virulence meets metabolism: Cra and KdpE gene regulation in enterohemorrhagic *Escherichia coli*. MBio **3:**e00280-00212.
72. **Porcheron G, Dozois CM.** 2015. Interplay between iron homeostasis and virulence: Fur and RyhB as major regulators of bacterial pathogenicity. Vet Microbiol **179:**2-14.
73. **Gorke B, Stulke J.** 2008. Carbon catabolite repression in bacteria: many ways to make the most out of nutrients. Nat Rev Microbiol **6:**613-624.
74. **Meibom KL, Charbit A.** 2010. *Francisella tularensi*s metabolism and its relation to virulence. Front Microbiol. **1:**140.
75. **Barel M, Charbit A.** 2013. *Francisella tularensis* intracellular survival: To eat or to die. Microbes Infect **pii:**S1286-4579(1213)00206-00202.
76. **Santic M, Abu Kwaik Y.** 2013. Nutritional virulence of *Francisella tularensis*. Front Cell Infect Microbiol **3:**112.
77. **Propst KL, Mima T, Choi KH, Dow SW, Schweizer HP.** 2010. A *Burkholderia pseudomallei* deltapurM mutant is avirulent in immunocompetent and immunodeficient animals: candidate strain for exclusion from select-agent lists. Infect Immun **78:**3136-3143.
78. **Norris MH, Propst KL, Kang Y, Dow SW, Schweizer HP, Hoang TT.** 2011. The *Burkholderia pseudomallei* Δasd mutant exhibits attenuated intracellular infectivity and imparts protection against acute inhalation melioidosis in mice. Infect Immun **79:**4010-4018.
79. **Rodrigues F, Sarkar-Tyson M, Harding SV, Sim SH, Chua HH, Lin CH, Han X, Karuturi RK, Sung K, Yu K, Chen W, Atkins TP, Titball RW, Tan P.** 2006. Global

map of growth-regulated gene expression in *Burkholderia pseudomallei*, the causative agent of melioidosis. J Bacteriol **188:**8178-8188.

80. **Korbsrisate S, Tomaras AP, Damnin S, Ckumdee J, Srinon V, Lengwehasatit I, Vasil ML, Suparak S.** 2007. Characterization of two distinct phospholipase C enzymes from *Burkholderia pseudomallei*. Microbiology **153:**1907-1915.
81. **Ireland PM, McMahon RM, Marshall LE, Halili M, Furlong E, Tay S, Martin JL, Sarkar-Tyson M.** 2014. Disarming *Burkholderia pseudomallei:* structural and functional characterization of a disulfide oxidoreductase (DsbA) required for virulence in vivo. Antioxid Redox Signal **20:**606-617.
82. **Drabner B, Guzmán CA.** 2001. Elicitation of predictable immune responses by using live bacterial vectors. Biomol Eng **17:**75-82.
83. **Peacock SJ, Limmathurotsakul D, Lubell Y, Koh GC, White LJ, Day NP, Titball RW.** 2012. Melioidosis vaccines: a systematic review and appraisal of the potential to exploit biodefense vaccines for public health purposes. PLoS Negl Trop Dis **6:**e1488.
84. **Butt AM, Tahir S, Nasrullah I, Idrees M, Lu J, Tong Y.** 2012. *Mycoplasma genitalium*: a comparative genomics study of metabolic pathways for the identification of drug and vaccine targets. Infect Genet Evol **12:**53-62.
85. **Butt AM, Nasrullah I, Tahir S, Tong Y.** 2012. Comparative genomics analysis of *Mycobacterium ulcerans* for the identification of putative essential genes and therapeutic candidates. PLoS One **7:**e43080.
86. **Anishetty S, Pulimi M, Pennathur G.** 2005. Potential drug targets in *Mycobacterium tuberculosis* through metabolic pathway analysis. Comput Biol Chem **29:**368-378.
87. **Yadav PK, Singh G, Singh S, Gautam B, Saad EI.** 2012. Potential therapeutic drug target identification in Community Acquired-Methicillin Resistant *Staphylococcus aureus* (CA-MRSA) using computational analysis. Bioinformation **8:**664-672.
88. **Uddin R, Saeed K.** 2014. Identification and characterization of potential drug targets by subtractive genome analyses of methicillin resistant *Staphylococcus aureus*. Comput Biol Chem **48:**55-63.
89. **Uddin R, Saeed K, Khan W, Azam SS, Wadood A.** 2015. Metabolic pathway analysis approach: Identification of novel therapeutic target against methicillin resistant *Staphylococcus aureus*. Gene **556:**213-226.
90. **Barh D, Tiwari S, Jain N, Ali A, Santos AR, Misra AN, Azevedo V, Kumar A.** 2011. In silico subtractive genomics for target identification in human bacterial pathogens. Drug Dev. Res. **72:**162-177.
91. **Ahn YY, Lee DS, Burd H, Blank W, Kapatral V.** 2014. Metabolic network analysis-based identification of antimicrobial drug targets in category A bioterrorism agents. PLoS One **9:**e85195.
92. **Damte D, Suh JW, Lee SJ, Yohannes SB, Hossain MA, Park SC.** 2013. Putative drug and vaccine target protein identification using comparative genomic analysis of KEGG annotated metabolic pathways of *Mycoplasma hyopneumoniae*. Genomics **102:**47-56.
93. **Fang K, Zhao H, Sun C, Lam CM, Chang S, Zhang K, Panda G, Godinho M, Martins dos Santos VA, Wang J.** 2011. Exploring the metabolic network of the epidemic pathogen *Burkholderia cenocepacia* J2315 via genome-scale reconstruction. BMC Syst Biol. **5:**83.
94. **Lee DS, Burd H, Liu J, Almaas E, Wiest O, Barabási AL, Oltvai ZN, Kapatral V.** 2009. Comparative genome-scale metabolic reconstruction and flux balance analysis of

multiple *Staphylococcus aureus* genomes identify novel antimicrobial drug targets. J Bacteriol. **191:**4015-4024.

95. **Rahman SA, Schomburg D.** 2006. Observing local and global properties of metabolic pathways: 'load points' and 'choke points' in the metabolic networks. Bioinformatics **22:**1767-1774.
96. **Baths V, Roy U, Singh T.** 2011. Disruption of cell wall fatty acid biosynthesis in *Mycobacterium tuberculosis* using a graph theoretic approach. Theor Biol Med Model **8:**5.
97. **Chaudhury S, Abdulhameed MD, Singh N, Tawa GJ, D'haeseleer PM, Zemla AT, Navid A, Zhou CE, Franklin MC, Cheung J, Rudolph MJ, Love J, Graf JF, Rozak DA, Dankmeyer JL, Amemiya K, Daefler S, Wallqvist A.** 2013. Rapid countermeasure discovery against Francisella tularensis based on a metabolic network reconstruction. PLoS One **8:**e63369.
98. **Heinemann M, Kümmel A, Ruinatscha R, Panke S.** 2005. In silico genome-scale reconstruction and validation of the *Staphylococcus aureus* metabolic network. Biotechnol Bioeng **92:**850-864.
99. **Herrgård MJ, Fong SS, Palsson BØ.** 2006. Identification of genome-scale metabolic network models using experimentally measured flux profiles. PLoS Comput Biol **2:**e72.
100. **Kim HU, Kim SY, Jeong H, Kim TY, Kim JJ, Choy HE, Yi KY, Rhee JH, Lee SY.** 2011. Integrative genome-scale metabolic analysis of *Vibrio vulnificus* for drug targeting and discovery. Mol Syst Biol **7:**460.
101. **Raghunathan A, Shin S, Daefler S.** 2010. Systems approach to investigating host-pathogen interactions in infections with the biothreat agent Francisella. Constraints-based model of *Francisella tularensis*. BMC Syst Biol **4:**118.
102. **Chavali AK, D'Auria KM, Hewlett EL, Pearson RD, Papin JA.** 2012. A metabolic network approach for the identification and prioritization of antimicrobial drug targets. Trends Microbiol. **20:**113-123.
103. **Fatumo S, Plaimas K, Mallm JP, Schramm G, Adebiyi E, Oswald M, Eils R, König R.** 2009. Estimating novel potential drug targets of *Plasmodium falciparum* by analysing the metabolic network of knock-out strains *in silico*. Infect Genet Evol **9:**351-358.
104. **Guimerà R, Sales-Pardo M, Amaral LA.** 2007. A network-based method for target selection in metabolic networks. Bioinformatics **23:**1616-1622.
105. **Chavali AK, Whittemore JD, Eddy JA, Williams KT, Papin JA.** 2008. Systems analysis of metabolism in the pathogenic trypanosomatid *Leishmania major*. Mol Syst Biol **4:**177.
106. **Perumal D, Lim CS, Sakharkar MK.** 2009. A Comparative Study of Metabolic Network Topology between a Pathogenic and a Non-Pathogenic Bacterium for Potential Drug Target Identification. Summit on Translat Bioinforma. **2009:**100-104.
107. **Taylor CM, Wang Q, Rosa BA, Huang SC, Powell K, Schedl T, Pearce EJ, Abubucker S, Mitreva M.** 2013. Discovery of anthelmintic drug targets and drugs using chokepoints in nematode metabolic pathways. PLoS Pathog **9:**e1003505.
108. **Ioerger TR, O'Malley T, Liao R, Guinn KM, Hickey MJ, Mohaideen N, Murphy KC, Boshoff HI, Mizrahi V, Rubin EJ, Sassetti CM, Barry CEr, Sherman DR, Parish T, Sacchettini JC.** 2013. Identification of new drug targets and resistance mechanisms in *Mycobacterium tuberculosis*. PLoS One **8:**e75245.

109. **Orelle C, Szal T, Klepacki D, Shaw KJ, Vázquez-Laslop N, Mankin AS.** 2013. Identifying the targets of aminoacyl-tRNA synthetase inhibitors by primer extension inhibition. Nucleic Acids Res **41:**e144.
110. **Novoa EM, Camacho N, Tor A, Wilkinson B, Moss S, Marín-García P, Azcárate IG, Bautista JM, Mirando AC, Francklyn CS, Varon S, Royo M, Cortés A, Ribas de Pouplana L.** 2014. Analogs of natural aminoacyl-tRNA synthetase inhibitors clear malaria in vivo. Proc Natl Acad Sci U S A. **111:**E5508-5517.
111. **Schimmel P, Tao J, Hill J.** 1998. Aminoacyl tRNA synthetases as targets for new anti-infectives. FASEB J **12:**1599-1609.
112. **Kim S, Lee SW, Choi EC, Choi SY.** 2003. Aminoacyl-tRNA synthetases and their inhibitors as a novel family of antibiotics. Appl Microbiol Biotechnol. **61:**278-288.
113. **Hurdle JG, O'Neill AJ, Chopra I.** 2005. Prospects for aminoacyl-tRNA synthetase inhibitors as new antimicrobial agents. Antimicrob Agents Chemother. **49:**4821-4833.
114. **Thomas CM, Hothersall J, Willis CL, Simpson TJ.** 2010. Resistance to and synthesis of the antibiotic mupirocin. Nat Rev Microbiol **8:**281-289.
115. **Koh CY, Siddaramaiah LK, Ranade RM, Nguyen J, Jian T, Zhang Z, Gillespie JR, Buckner FS, Verlinde CL, Fan E, Hol WG.** 2015. A binding hotspot in *Trypanosoma cruzi* histidyl-tRNA synthetase revealed by fragment-based crystallographic cocktail screens. Acta Crystallogr D Biol Crystallogr **71:**1684-1698.
116. **Biela I, Tidten-Luksch N, Immekus F, Glinca S, Nguyen TX, Gerber HD, Heine A, Klebe G, Reuter K.** 2013. Investigation of specificity determinants in bacterial tRNA-guanine transglycosylase reveals queuine, the substrate of its eucaryotic counterpart, as inhibitor. PLoS One **8:**e64240.
117. **Grädler U, Gerber HD, Goodenough-Lashua DM, Garcia GA, Ficner R, Reuter K, Stubbs MT, Klebe G.** 2001. A new target for shigellosis: rational design and crystallographic studies of inhibitors of tRNA-guanine transglycosylase. J Mol Biol **306:**455-467.
118. **Pohlhaus JR, Long DT, O'Reilly E, Kreuzer KN.** 2008. The epsilon subunit of DNA polymerase III Is involved in the nalidixic acid-induced SOS response in *Escherichia coli*. J Bacteriol **190:**5239-5247.
119. **Cirz RT, Chin JK, Andes DR, de Crécy-Lagard V, Craig WA, Romesberg FE.** 2005. Inhibition of Mutation and Combating the Evolution of Antibiotic Resistance. PLoS Biology **3:**e176.
120. **Nautiyal A, Patil KN, Muniyappa K.** 2014. Suramin is a potent and selective inhibitor of *Mycobacterium tuberculosis* RecA protein and the SOS response: RecA as a potential target for antibacterial drug discovery. J Antimicrob Chemother **69:**1834-1843.
121. **Culyba MJ, Mo CY, Kohli RM.** 2015. Targets for Combating the Evolution of Acquired Antibiotic Resistance. Biochemistry **54:**3573-3582.
122. **Tye B-K, Lehman IR.** 1977. Excision repair of uracil incorporated in DNA as a result of a defect in dUTPase. J. Mol. Biol. **117:**293–306.
123. **Nguyen C, Kasinathan G, Leal-Cortijo I, Musso-Buendia A, Kaiser M, Brun R, Ruiz-Pérez LM, Johansson NG, González-Pacanowska D, Gilbert IH.** 2005. Deoxyuridine triphosphate nucleotidohydrolase as a potential antiparasitic drug target. J Med Chem **48:**5942-5954.
124. **Hampton SE, Baragaña B, Schipani A, Bosch-Navarrete C, Musso-Buendía JA, Recio E, Kaiser M, Whittingham JL, Roberts SM, Shevtsov M, Brannigan JA,**

Kahnberg P, Brun R, Wilson KS, González-Pacanowska D, Johansson NG, Gilbert IH. 2011. Design, synthesis, and evaluation of 5'-diphenyl nucleoside analogues as inhibitors of the *Plasmodium falciparum* dUTPase. ChemMedChem **6:**1816-1831.

125. **Kepple KV, Boldt JL, Segall AM.** 2005. Holliday junction-binding peptides inhibit distinct junction-processing enzymes. Proc Natl Acad Sci U S A **102:**6867-6872.
126. **Sechman EV, Kline KA, Seifert S.** 2006. Loss of both Holliday junction processing pathways is synthetically lethal in the presence of gonococcal pilin antigenic variation. Mol Microbiol **61:**185-193.
127. **Suksangpleng T, Leartsakulpanich U, Moonsom S, Siribal S, Boonyuen U, Wright GE, Chavalitshewinkoon-Petmitr P.** 2014. Molecular characterization of *Plasmodium falciparum* uracil-DNA glycosylase and its potential as a new anti-malarial drug target. Malar J **13:**149.
128. **Venkatesh J, Kumar P, Krishna PS, Manjunath R, Varshney U.** 2003. Importance of uracil DNA glycosylase in *Pseudomonas aeruginosa* and *Mycobacterium smegmatis*, G+C-rich bacteria, in mutation prevention, tolerance to acidified nitrite, and endurance in mouse macrophages. . J Biol Chem. **278:**24350-24358.
129. **Landini P, Corti E, Goldstein BP, Denaro M.** 1992. Mechanism of action of purpuromycin. Biochem J **284:**47-52.
130. **Nishio A, Uyeki EM.** 1983. Cellular uptake and inhibition of DNA synthesis by dihydroxyanthraquinone and two analogues. Cancer Res **43:**1951-1956.
131. **Kelly TM, Stachula SA, Raetz CR, Anderson MS.** 1993. The firA gene of *Escherichia coli* encodes UDP-3-O-(R-3-hydroxymyristoyl)-glucosamine N-acyltransferase. The third step of endotoxin biosynthesis. J Biol Chem. **268:**19866-19874.
132. **Raetz CR, Whitfield C.** 2002. Lipopolysaccharide endotoxins. Annu Rev Biochem **71:**635-700.
133. **Emiola A, George J, Andrews SS.** 2015. A Complete Pathway Model for Lipid A Biosynthesis in *Escherichia coli*. PLoS One **10:**e0121216.
134. **Farha MA, Czarny TL, Myers CL, Worrall LJ, French S, Conrady DG, Wang Y, Oldfield E, Strynadka NC, Brown ED.** 2015. Antagonism screen for inhibitors of bacterial cell wall biogenesis uncovers an inhibitor of undecaprenyl diphosphate synthase. Proc Natl Acad Sci U S A **112:**11048-11053.
135. **Dodbele S, Martinez CD, Troutman JM.** 2014. Species differences in alternative substrate utilization by the antibacterial target undecaprenyl pyrophosphate synthase. Biochemistry **53:**5042-5050.
136. **Kuo CJ, Guo RT, Lu IL, Liu HG, Wu SY, Ko TP, Wang AH, Liang PH.** 2008. Structure-based inhibitors exhibit differential activities against Helicobacter pylori and Escherichia coli undecaprenyl pyrophosphate synthases. J Biomed Biotechnol **2008:**841312.
137. **Zhu W, Zhang Y, Sinko W, Hensler ME, Olson J, Molohon KJ, Lindert S, Cao R, Li K, Wang K, Wang Y, Liu YL, Sankovsky A, de Oliveira CA, Mitchell DA, Nizet V, McCammon JA, Oldfield E.** 2013. Antibacterial drug leads targeting isoprenoid biosynthesis. Proc Natl Acad Sci U S A **110:**123-128.
138. **Sinko W, Wang Y, Zhu W, Zhang Y, Feixas F, Cox CL, Mitchell DA, Oldfield E, McCammon J.** 2014. Undecaprenyl diphosphate synthase inhibitors: antibacterial drug leads. J Med Chem **57:**5693-5701.

139. **Walker S, Chen L, Hu Y, Rew Y, Shin D, Boger DL.** 2005. Chemistry and biology of ramoplanin: a lipoglycodepsipeptide with potent antibiotic activity. Chem Rev **105:**449-476.
140. **Helm JS, Hu Y, Chen L, Gross B, Walker S.** 2003. Identification of active-site inhibitors of MurG using a generalizable, high-throughput glycosyltransferase screen. J Am Chem Soc **125:**11168-11169.
141. **Mann PA, Müller A, Xiao L, Pereira PM, Yang C, Ho Lee S, Wang H, Trzeciak J, Schneeweis J, Dos Santos MM, Murgolo N, She X, Gill C, Balibar CJ, Labroli M, Su J, Flattery A, Sherborne B, Maier R, Tan CM, Black T, Onder K, Kargman S, Monsma FJJ, Pinho MG, Schneider T, Roemer T.** 2013. Murgocil is a highly bioactive staphylococcal-specific inhibitor of the peptidoglycan glycosyltransferase enzyme MurG. ACS Chem Biol **8:**2442-2451.
142. **Olesen SH, Ingles DJ, Yang Y, Schönbrunn E.** 2014. Differential antibacterial properties of the MurA inhibitors terreic acid and fosfomycin. J Basic Microbiol **54:**322-326.
143. **Bensen DC, Rodriguez S, Nix J, Cunningham ML, Tari LW.** 2012. Structure of MurA (UDP-N-acetylglucosamine enolpyruvyl transferase) from *Vibrio fischeri* in complex with substrate UDP-N-acetylglucosamine and the drug fosfomycin. Acta Crystallogr Sect F Struct Biol Cryst Commun **68:**382-385.
144. **Gautam A, Rishi P, Tewari R.** 2011. UDP-N-acetylglucosamine enolpyruvyl transferase as a potential target for antibacterial chemotherapy: recent developments. Appl Microbiol Biotechnol. **92:**211-212.
145. **Han H, Yang Y, Olesen SH, Becker A, Betzi S, Schönbrunn E.** 2010. The fungal product terreic acid is a covalent inhibitor of the bacterial cell wall biosynthetic enzyme UDP-N-acetylglucosamine 1-carboxyvinyltransferase (MurA) Biochemistry **49:**4276-4282.
146. **Bachelier A, Mayer R, Klein CD.** 2006. Sesquiterpene lactones are potent and irreversible inhibitors of the antibacterial target enzyme MurA. Bioorg Med Chem Lett **16:**5605-5609.
147. **Eschenburg S, Priestman MA, Abdul-Latif FA, Delachaume C, Fassy F, Schönbrunn E.** 2005. A novel inhibitor that suspends the induced fit mechanism of UDP-N-acetylglucosamine enolpyruvyl transferase (MurA). J Biol Chem. **280:**14070-14075.
148. **Smithen DA, Forget SM, McCormick NE, Syvitski RT, Jakeman DL.** 2015. Polyphosphate-containing bisubstrate analogues as inhibitors of a bacterial cell wall thymidylyltransferase. Org Biomol Chem **13:**3347-3350.
149. **Blankenfeldt W, Asuncion M, Lam JS, Naismith JH.** 2000. The structural basis of the catalytic mechanism and regulation of glucose-1-phosphate thymidylyltransferase (RmlA). EMBO J **19:**6652-6663.
150. **Lakhal-Naouar I, Jardim A S, R., Luo S K, Y., Nakhasi HL, Duncan RC.** 2012. *Leishmania donovani* argininosuccinate synthase is an active enzyme associated with parasite pathogenesis. PLoS Negl Trop Dis. **6:**e1849.
151. **Piet JR, Geldhoff M, van Schaik BD, Brouwer MC, Valls Seron M, Jakobs ME, Schipper K, Pannekoek Y, Zwinderman AH, van der Poll T, van Kampen AH, Baas F, van der Ende A, van de Beek D.** 2014. *Streptococcus pneumoniae* arginine synthesis

genes promote growth and virulence in pneumococcal meningitis. J Infect Dis. **209:**1781-1791.
152. **Somvanshi VS, Viswanathan P, Jacobs JL, Mulks MH, Sundin GW, Ciche TA.** 2010. The type 2 secretion Pseudopilin, gspJ, is required for multihost pathogenicity of *Burkholderia cenocepacia* AU1054. Infect Immun. **78:**4110-4121.
153. **Yang HL, Kessler DP.** 1974. Genetic analysis of the leucine region in *Escherichia coli* B-r: gene-enzyme assignments. J Bacteriol **117:**63-72.
154. **Singh RK, Kefala G, Janowski R, Mueller-Dieckmann C, von Kries JP, Weiss MS.** 2005. The high-resolution Structure of LeuB (Rv2995c) from *Mycobacterium tuberculosis*. J Mol Biol. **346:**1-11.
155. **Pettit FH, Reed LJ.** 1967. Alpha-keto acid dehydrogenase complexes. 8. Comparison of dihydrolipoyl dehydrogenases from pyruvate and alpha-ketoglutarate dehydrogenase complexes of *Escherichia coli*. Proc Natl Acad Sci U S A. **58:**1126-1130.
156. **Bryk R, Arango N, Maksymiuk C, Balakrishnan A, Wu YT, Wong CH, Masquelin T, Hipskind P, Lima CD, Nathan C.** 2013. Lipoamide channel-binding sulfonamides selectively inhibit mycobacterial lipoamide dehydrogenase. Biochemistry **52:**9375-9384.
157. **Krauth-Siegel RL, Schöneck R.** 1995. Flavoprotein structure and mechanism. 5. Trypanothione reductase and lipoamide dehydrogenase as targets for a structure-based drug design. FASEB J **9:**1138-1146.
158. **Boitz JM, Strasser R, Yates PA, Jardim A, Ullman B.** 2013. Adenylosuccinate synthetase and adenylosuccinate lyase deficiencies trigger growth and infectivity deficits in *Leishmania donovani*. J Biol Chem. **288:**8977-8990.
159. **Howard NI, Dias MV, Peyrot F, Chen L, Schmidt MF, Blundell TL, Abell C.** 2015. Design and structural analysis of aromatic inhibitors of type II dehydroquinase from *Mycobacterium tuberculosis*. ChemMedChem **10:**116-133.
160. **Cheung VW, Xue B, Hernandez-Valladares M, Go MK, Tung A, Aguda AH, Robinson RC, Yew WS.** 2014. Identification of polyketide inhibitors targeting 3-dehydroquinate dehydratase in the shikimate pathway of *Enterococcus faecalis*. PLoS One **9:**e103598.
161. **Ballester PJ, Mangold M, Howard NI, Robinson RL, Abell C, Blumberger J, Mitchell JB.** 2012. Hierarchical virtual screening for the discovery of new molecular scaffolds in antibacterial hit identification. J R Soc Interface **9:**3196-3207.
162. **Kumar A, Siddiqi MI, Miertus S.** 2010. New molecular scaffolds for the design of *Mycobacterium tuberculosis* type II dehydroquinase inhibitors identified using ligand and receptor based virtual screening. J Mol Model **16:**693-712.
163. **Prazeres VF, Sánchez-Sixto C, Castedo L, Lamb H, Hawkins A, R., Riboldi-Tunnicliffe A, Coggins JR, Lapthorn AJ, González-Bello C.** 2007. Nanomolar competitive inhibitors of *Mycobacterium tuberculosis* and *Streptomyces coelicolor* type II dehydroquinase. ChemMedChem **2:**194-207.
164. **Siggaard-Andersen M, Wissenbach M, Chuck JA, Svendsen I, Olsen JG, von Wettstein-Knowles P.** 1994. The fabJ-encoded beta-ketoacyl-[acyl carrier protein] synthase IV from *Escherichia coli* is sensitive to cerulenin and specific for short-chain substrates. Proc Natl Acad Sci U S A. **91:**11027-11031.
165. **Magnuson K, Carey MR, Cronan JEJ.** 1995. The putative fabJ gene of *Escherichia coli* fatty acid synthesis is the fabF gene. J Bacteriol **177:**3593-3595.

166. **Tong L.** 2013. Structure and function of biotin-dependent carboxylases. Cell Mol Life Sci **70:**863-891.
167. **Silvers MA, Robertson GT, Taylor CM, Waldrop GL.** 2014. Design, synthesis, and antibacterial properties of dual-ligand inhibitors of acetyl-CoA carboxylase. J Med Chem **57:**8947-8959.
168. **Reddy MC, Breda A, Bruning JB, Sherekar M, Valluru S, Thurman C, Ehrenfeld H, Sacchettini JC.** 2014. Structure, activity, and inhibition of the Carboxyltransferase β-subunit of acetyl coenzyme A carboxylase (AccD6) from *Mycobacterium tuberculosis*. Antimicrob Agents Chemother **58:**6122-6132.
169. **Levert KL, Waldrop GL.** 2002. A bisubstrate analog inhibitor of the carboxyltransferase component of acetyl-CoA carboxylase. Biochem Biophys Res Commun **291:**1213-1217.
170. **Freiberg C, Brunner NA, Schiffer G, Lampe T, Pohlmann J, Brands M, Raabe M, Häbich D, Ziegelbauer K.** 2004. Identification and characterization of the first class of potent bacterial acetyl-CoA carboxylase inhibitors with antibacterial activity. J Biol Chem. **279:**26066-26073.
171. **Tong L.** 2005. Acetyl-coenzyme A carboxylase: crucial metabolic enzyme and attractive target for drug discovery. Cell Mol Life Sci **62:**1784-1803.
172. **Zhang R, Ou HY, Zhang CT.** 2004. DEG: a database of essential genes. Nucleic Acids Res **32(Database issue):**D271-272.
173. **Moule MG, Hemsley CM, Seet Q, Guerra-Assunção JA, Lim J, Sarkar-Tyson M, Clark TG, Tan PB, Titball RW, Cuccui J, Wren BW.** 2014. Genome-wide saturation mutagenesis of *Burkholderia pseudomallei* K96243 predicts essential genes and novel targets for antimicrobial development. MBio **5:**e00926-00913.
174. **Somvanshi VS, Viswanathan P, Jacobs JL, Mulks MH, Sundin GW, Ciche TA.** 2010. The type 2 secretion Pseudopilin, gspJ, is required for multihost pathogenicity of *Burkholderia cenocepacia* AU1054. Infect Immun **78:**4110-4121.
175. **van Waasbergen LG, Kidambi SP, Miller RV.** 1998. Construction of a recA mutant of *Burkholderia* (formerly Pseudomonas), *cepacia*. Appl Microbiol Biotechnol **49:**59-65.
176. **Appleberg R.** 2006. Macrophage nutriprive antimicrobial mechanisms. J Leukocyte Biol **70:**1117-1128.
177. **McKinney JD, Bentrup KH, Mun˜ oz-Elias EJ, Miczak A, Chen B, Chan WT, Swenson D, Sacchettini JC, Jacobs Jr. WR, Russell DG.** 2000. Persistence of *Mycobacterium tuberculosis* in macrophages and mice requires the glyoxylate shunt enzyme isocitrate lyase. Nature **406:**735–738.
178. **Fang FC, Libby SJ, Castor ME, Fung AM.** 2005. Isocitrate lyase (AceA) is required for Salmonella persistence but not for acute lethal infection in mice. Infect. Immun. **73:**2547–2549.
179. **Liu N, Cummings JE, England K, Slayden RA, Tonge PJ.** 2011. Mechanism and inhibition of the FabI enoyl-ACP reductase from *Burkholderia pseudomallei*. J Antimicrob Chemother **66:**564-573.
180. **Bokman AH, Levine HB, Lusby M.** 1957. Glucose catabolism in *Malleomyces pseudomallei*. J Bacteriol **73:**649-654.
181. **Kouassi Y, Shelef LA.** 1996. Metabolic activities of *Listeria monocytogenes* in the presence of sodium propionate, acetate, lactate and citrate. J Appl Bacteriol **81:**147-153.

182. **Premaratne RJ, Lin WJ, Johnson EA.** 1991. Development of an improved chemically defined minimal medium for *Listeria monocytogenes*. Appl Environ Microbiol. **57:**3046-3048.
183. **Joseph B, Przybilla K, Stühler C, Schauer K, Slaghuis J, Fuchs TM, Goebel W.** 2006. Identification of *Listeria monocytogenes* genes contributing to intracellular replication by expression profiling and mutant screening. J Bacteriol. **188:**556-568.
184. **Bordbar A, Lewis NE, Schellenberger J, Palsson BØ, Jamshidi N.** 2010. Insight into human alveolar macrophage and *M. tuberculosis* interactions via metabolic reconstructions. Mol Syst Biol **6:**422.
185. **Chatterjee SS, Hossain H, Otten S, Kuenne C, Kuchmina K, Machata S, Domann E, Chakraborty T, Hain T.** 2006. Intracellular gene expression profile of *Listeria monocytogenes*. Infect Immun **74:**1323-1338.
186. **Eisenreich W, Heesemann J, Rudel T, Goebel W.** 2013. Metabolic host responses to infection by intracellular bacterial pathogens. Front Cell Infect Microbiol **3:**24.
187. **Caspi R, Altman T, Dale JM, Dreher K, Fulcher CA, Gilham F, Kaipa P, Karthikeyan AS, Kothari A, Krummenacker M, Latendresse M, Mueller LA, Paley S, Popescu L, Pujar A, Shearer AG, Zhang P, Karp PD.** 2010. The MetaCyc database of metabolic pathways and enzymes and the BioCyc collection of pathway/genome databases. Nucleic Acids Res. **38(Database issue):**D473-479.
188. **Joseph B, Przybilla K, Stühler C, Schauer K, Slaghuis J, Fuchs TM, Goebel W.** 2006. Identification of *Listeria monocytogenes* genes contributing to intracellular replication by expression profiling and mutant screening. J Bacteriol.**:**556-568.
189. **Tuanyok A, Tom M, Dunbar J, Woods DE.** 2006. Genome-wide expression analysis of Burkholderia pseudomallei infection in a hamster model of acute melioidosis. Infect Immun **74:**5465-5476.
190. **Hamad MA, Austin CR, Stewart AL, Higgins M, Vázquez-Torres A, Voskuil MI.** 2011. Adaptation and antibiotic tolerance of anaerobic *Burkholderia pseudomallei*. Antimicrob Agents Chemother **55:**3313-3323.
191. **van Schaik E, Tom M, DeVinney R, Woods DE.** 2008. Development of novel animal infection models for the study of acute and chronic *Burkholderia pseudomallei* pulmonary infections. Microbes Infect **10:**1291-1299.
192. **Alberts B, Johnson A, Lewis J, Raff M, Roberts K, Walter P.** 2002. Molecular Biology of the Cell, 4th edition. Garland Science, New York.
193. **Myint KT, Uehara T, Aoshima K, Oda Y.** 2009. Polar anionic metabolome analysis by nano-LC/MS with a metal chelating agent. Anal Chem **81:**7766-7772.
194. **Lee IJ, Hom K, Bai G, Shapiro M.** 2009. NMR metabolomic analysis of caco-2 cell differentiation. J Proteome Res **8:**4104-4108.

Figure 1. Metabolic pathways in *B. pseudomallei* MSHR668 that show reduced flux when chokepoint enzymes (indicated by pink arrows) are deleted *in silico*. **A.** The mono-trans, poly-cis decaprenyl phosphate biosynthesis pathway that contains the chokepoint enzyme undecaprenyl diphosphate synthase (*uppS*). **B**. The two chokepoints UDP-N-acetylglucosamine--N-acetylmuramyl-(pentapeptide) pyrophosphoryl-decaprenol N-acetylglucosamine transferase (*murG*) and UDP-3-O-(R-3-hydroxymyristoyl)-glucosamine N-acyltransferase (*lpxD*), involved in peptidoglycan and lipid A biosynthesis, respectively. **C.** The 3-isopropylmalate dehydrogenase (*leuB*) chokepoint enzyme performs the third step in leucine biosynthesis. **D.** The chokepoint enzyme tRNA-guanine transglycosylase (*tgt*), involved in queosine biosynthesis. *In silico* deletion of UDP-3-O-(R-3-hydroxymyristoyl)-glucosamine N-acyltransferase (*lpxD*) reduced flux through the *B. pseudomallei* metabolic network in the LB media model, deletion of undecaprenyl diphosphate synthase (*uppS*) reduced flux through both unconstrained and LB media models, and deletion of tRNA-guanine transglycosylase (*tgt*) and 3-isopropylmalate dehydrogenase (*leuB*) reduced flux in the unconstrained model. These pathways were rendered by the Cellular Overview feature of Pathway Tools.

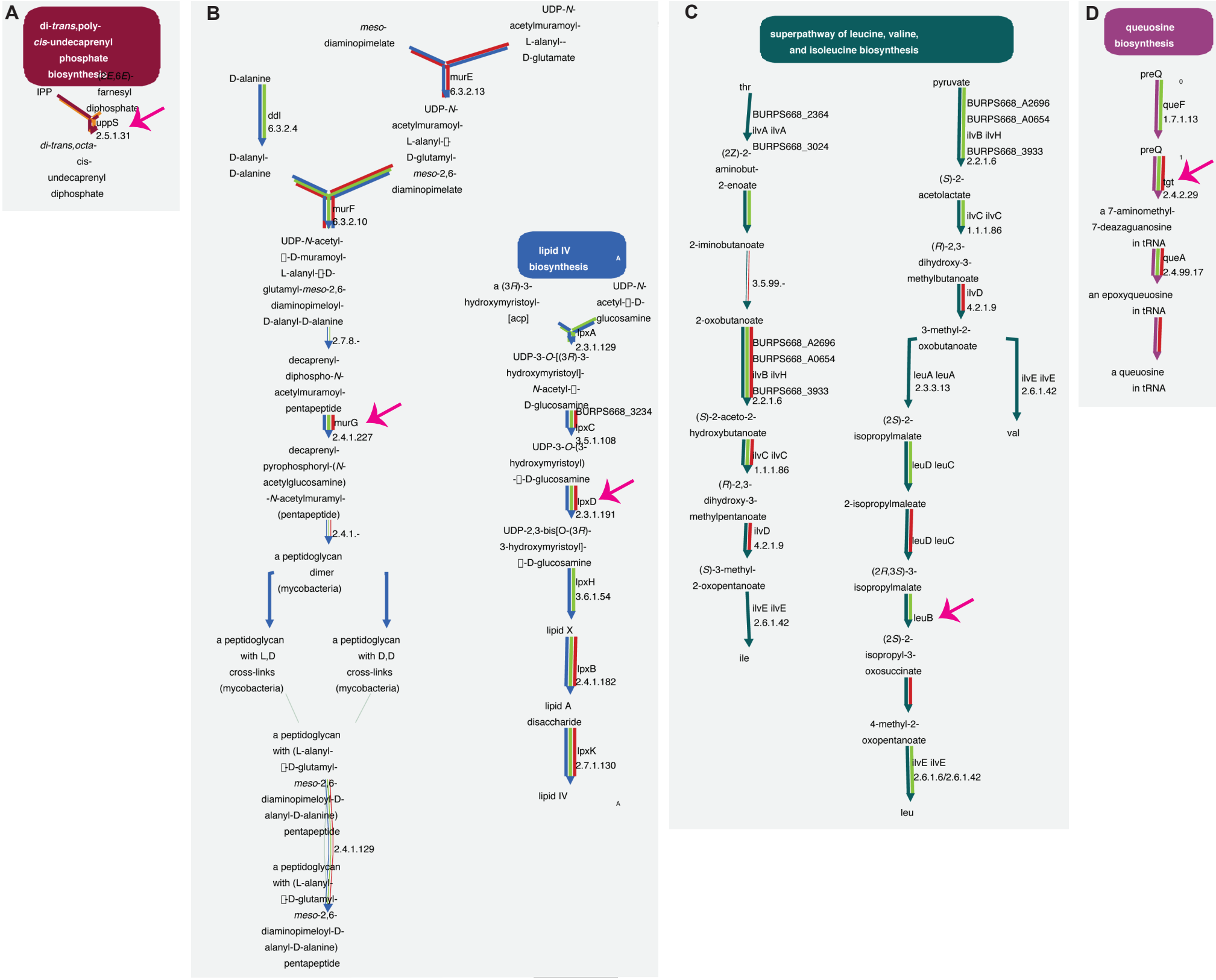
A
di-trans,poly-cis-undecaprenyl phosphate biosynthesis
IPP
(2E,6E)-farnesyl diphosphate
uppS
2.5.1.31
di-trans,octa-cis-undecaprenyl diphosphate
B
meso-diaminopimelate
UDP-N-acetylmuramoyl-L-alanyl--D-glutamate
murE
6.3.2.13
D-alanine
ddl
6.3.2.4
D-alanyl-D-alanine
UDP-N-acetylmuramoyl-L-alanyl-D-glutamyl-meso-2,6-diaminopimelate
murF
6.3.2.10
UDP-N-acetyl-D-muramoyl-L-alanyl-D-glutamyl-meso-2,6-diaminopimeloyl-D-alanyl-D-alanine
2.7.8.-
decaprenyl-diphospho-N-acetylmuramoyl-pentapeptide
murG
2.4.1.227
decaprenyl-pyrophosphoryl-(N-acetylglucosamine)-N-acetylmuramyl-(pentapeptide)
2.4.1.-
a peptidoglycan dimer (mycobacteria)
a peptidoglycan with L,D cross-links (mycobacteria)
a peptidoglycan with D,D cross-links (mycobacteria)
a peptidoglycan with (L-alanyl-D-glutamyl-meso-2,6-diaminopimeloyl-D-alanyl-D-alanine) pentapeptide
2.4.1.129
a peptidoglycan with (L-alanyl-D-glutamyl-meso-2,6-diaminopimeloyl-D-alanyl-D-alanine) pentapeptide
lipid IV biosynthesis
a (3R)-3-hydroxymyristoyl-[acp]
UDP-N-acetyl-D-glucosamine
lpxA
2.3.1.129
UDP-3-O-[(3R)-3-hydroxymyristoyl]-N-acetyl-D-glucosamine
BURPS668_3234
lpxC
3.5.1.108
UDP-3-O-(3-hydroxymyristoyl)-D-glucosamine
lpxD
2.3.1.191
UDP-2,3-bis[O-(3R)-3-hydroxymyristoyl]-D-glucosamine
lpxH
3.6.1.54
lipid X
lpxB
2.4.1.182
lipid A disaccharide
lpxK
2.7.1.130
lipid IV
C
superpathway of leucine, valine, and isoleucine biosynthesis
thr
BURPS668_2364
ilvA ilvA
BURPS668_3024
(2Z)-2-aminobut-2-enoate
2-iminobutanoate
3.5.99.-
2-oxobutanoate
BURPS668_A2696
BURPS668_A0654
ilvB ilvH
BURPS668_3933
2.2.1.6
(S)-2-aceto-2-hydroxybutanoate
ilvC ilvC
1.1.1.86
(R)-2,3-dihydroxy-3-methylpentanoate
ilvD
4.2.1.9
(S)-3-methyl-2-oxopentanoate
ilvE ilvE
2.6.1.42
ile
pyruvate
BURPS668_A2696
BURPS668_A0654
ilvB ilvH
BURPS668_3933
2.2.1.6
(S)-2-acetolactate
ilvC ilvC
1.1.1.86
(R)-2,3-dihydroxy-3-methylbutanoate
ilvD
4.2.1.9
3-methyl-2-oxobutanoate
leuA leuA
2.3.3.13
ilvE ilvE
2.6.1.42
val
(2S)-2-isopropylmalate
leuD leuC
2-isopropylmaleate
leuD leuC
(2R,3S)-3-isopropylmalate
leuB
(2S)-2-isopropyl-3-oxosuccinate
4-methyl-2-oxopentanoate
ilvE ilvE
2.6.1.6/2.6.1.42
leu
D
queuosine biosynthesis
preQ0
queF
1.7.1.13
preQ1
tgt
2.4.2.29
a 7-aminomethyl-7-deazaguanosine in tRNA
queA
2.4.99.17
an epoxyqueuosine in tRNA
a queuosine in tRNA